Received: 13 April 2023 | Revised: 27 September 2023 | Accepted: 6 October 2023

DOI: 10.1002/nla.2536

SPECIAL ISSUE PAPER

WILEY

Algebra preconditionings for 2D Riesz distributed-order space-fractional diffusion equations on convex domains

Mariarosa Mazza[1,2] | **Stefano Serra-Capizzano**[2,3] | **Rosita Luisa Sormani**[4]

[1]Department of Mathematics, Università di Roma Tor Vergata, Rome, Italy

[2]Department of Science and High Technology, University of Insubria, INDAM Unit, Como, Italy

[3]Department of Information Technology, Uppsala University, Uppsala, Sweden

[4]Department of Theoretical and Applied Sciences, University of Insubria, Varese, Italy

Correspondence
Rosita Luisa Sormani, Department of Theoretical and Applied Sciences, University of Insubria, Via Dunant 3, 21100, Varese, Italy.
Email: rl.sormani@uninsubria.it

Funding information
European High-Performance Computing Joint Undertaking, Grant/Award Number: 955701; European Union's Horizon 2020 Research and Innovation Program; Gruppo Nazionale per il Calcolo Scientifico, Grant/Award Number: CUP E53C22001930001; Laboratory of Theory, Economics and Systems - Department of Computer Science at Athens University of Economics and Business

Abstract

When dealing with the discretization of differential equations on non-rectangular domains, a careful treatment of the boundary is mandatory and may result in implementation difficulties and in coefficient matrices without a prescribed structure. Here we examine the numerical solution of a two-dimensional constant coefficient distributed-order space-fractional diffusion equation with a nonlinear term on a convex domain. To avoid the aforementioned inconvenience, we resort to the volume-penalization method, which consists of embedding the domain into a rectangle and in adding a reaction penalization term to the original equation that dominates in the region outside the original domain and annihilates the solution correspondingly. Thanks to the volume-penalization, methods designed for problems in rectangular domains are available for those in convex domains and by applying an implicit finite difference scheme we obtain coefficient matrices with a 2-level Toeplitz structure plus a diagonal matrix which arises from the penalty term. As a consequence of the latter, we can describe the asymptotic eigenvalue distribution as the matrix size diverges as well as estimate the intrinsic asymptotic ill-conditioning of the involved matrices. On these bases, we discuss the performances of the conjugate gradient with circulant and τ-preconditioners and of the generalized minimal residual with split circulant and τ-preconditioners and conduct related numerical experiments.

KEYWORDS

matrix-sequences, optimality, preconditioned Krylov methods, spectral analysis

1 | INTRODUCTION

Fractional diffusion equations (FDEs) have attracted growing attention in the last decades, due to the fact that they represent a powerful tool for modeling anomalous diffusion that arises in a wide range of applicative fields.[1-4] Their versatility relies on the fractional derivative order, a noninteger parameter that can be calibrated to model enhanced diffusivity, overcoming the limits of classical integer order modeling (see the book by Podlubny[4] and references therein). Particularly effective in portraying anomalous diffusion are the so-called distributed-order operators, where the fractional derivative is integrated with respect to the order of differentiation, within a given range. They arise when the fractional

Dedicated to Prof. Owe Axelsson, to his scientific talent, to his ethical approach to science, to his continuous help to younger researchers.

order varies continuously in the interior of the domain. This results in a sum of the contributions over the domain, leading to an integral over the order parameter.[1,2] Applications of the fractional distributed order paradigma in porous media and groundwater flow can be found in the literature.[5,6] Since analytical solutions for FDEs are rarely available, the investigation of numerical methods for the computation of approximate solutions constitutes an active and promising field of research.

In the present work, we focus on a semi-linear two-dimensional Riesz distributed-order space-FDE defined on a convex domain. A linear version of this problem was discretized by means of a finite element method over unstructured/non-Cartesian meshes.[7] The versatility of this method comes at a price as the boundary treatment asks for some extra care and the resulting coefficient matrices do not have a distinct structure. To avoid these drawbacks, we adopt a different strategy. Rather than adjusting the discretization, we act on the continuous problem and alter it in a way that allows us to employ uniform grids and therefore preserve the good structure of the matrices. More precisely, we resort to the volume-penalization method,[8] applied by Huang and Sun to solve a semi-linear Riesz space FDE.[9] Such technique consists in embedding the domain into a rectangle and considering an extended problem with an additional reaction penalization term, that dominates outside of the original domain and serves the purpose of annihilating the solution correspondingly. The latter purpose is achieved by introducing a penalization parameter that, as it tends to zero, magnifies the reaction term over the fractional differential operator and forces the solution to be zero outside of the original domain. The idea of embedding the domain in a rectangle and then using a suitable reformulation of the problem is the common denominator of the large class of *immersed methods* (see e.g., References 10,11 and references therein), whose starting point is quite old and indeed these methods intersect with those called *fictitious domain methods*.[12,13]

Thus, we obtain a problem on a rectangular domain that can be discretized on uniform grids. In particular, we adopt a second-order finite difference method for time derivative and a weighted and shifted Grünwald–Letnikov difference scheme for the fractional derivatives, combined with a quadrature rule for the integral and an approximation for the nonlinear term derived from Taylor expansions. The overall numerical scheme has a second-order convergence in both time and space directions. In addition, the presence of uniform gridding results in 2-level Toeplitz matrices, due to the shift-invariant nature of the operators, plus a diagonal matrix arising from the penalty term. This is crucial for overcoming the disadvantages of having full coefficient matrices, which in general require $\mathcal{O}(n^3)$ computational costs and $\mathcal{O}(n^2)$ storage costs, where n is the number of grid points. In fact, the storage requirement for a Toeplitz structure amounts only to $\mathcal{O}(n)$ and the complexity of the matrix-vector product is reduced to $\mathcal{O}(n \log n)$ thanks to the use of the fast Fourier transform (FFT).

Moreover, putting together the matrices obtained for each discretization step, we obtain a real symmetric structured matrix-sequence, which can be associated to a function, called (spectral) symbol, and asymptotically representing the distribution of the eigenvalues as the matrix size increases. We recall that the evaluation of the symbol over an equispaced grid leads to a reasonable approximation of the eigenvalues, when the size of the matrix is sufficiently large. Applying the well-known theory of Toeplitz and generalized locally Toeplitz sequences,[14] and building on the information available regarding the one-dimensional case,[15] we are able to explicitly compute the symbol of the (properly scaled) coefficient matrix-sequence and exploit the spectral information in order to design preconditioners that counterbalance the asymptotic ill-conditioning.

The first preconditioner we investigate consists in a two-level version of the τ-preconditioners described in detail in the one-dimensional setting.[15] As a basis for comparison, we consider a two-level Strang-type circulant preconditioner. Aware of the negative results regarding the convergence rate of matrix-algebra preconditioning in a multilevel setting,[16,17] we cannot expect either superlinear or mesh independent convergence in general. However, the τ-preconditioner is a preferable option in the real symmetric setting,[18] especially because of a substantially better matching of the small eigenvalues (an application to fractional problems has been investigated[19]). However, both preconditioners do not include the diagonal matrix arising from the penalty term and this could cause poor performances of the preconditioned conjugate gradient (PCG). Therefore, as a second preconditioner we study an adaptation to the distributed case of a split τ-preconditioner[9] proposed for a non-distributed problem. A circulant version of the split preconditioner is also taken into account. These preconditioners are non-symmetric, therefore the associated linear systems need to be solved via the generalized minimal residual (GMRES) method. Moreover, they require two extra fast transforms if compared with the non-split circulant and τ-preconditioners. For all the aforementioned preconditioners, we compute the symbol and exploit the spectral information to assess which preconditioners should be the preferable choice under different circumstances. The numerical tests emphasize that both τ-preconditioners need fewer iterations than their circulant versions and this is in line with the theoretical results. Moreover, if the penalization parameter is small enough, the split preconditioners typically provide a lower number of iterations, which balances the higher cost of the GMRES method compared to the PCG and the two extra fast transforms.

The current paper is organized as follows. Section 2 introduces the continuous problem, its extension with the volume-penalization method and the discretization, including the basic features of the resulting coefficient matrices. Section 3 is devoted to the calculation of the symbol and the spectral analysis. Section 4 contains the preconditioning proposal and the spectral study of the preconditioners, followed in Section 5 by the discussion of several numerical experiments. Finally, in Section 6 we draw conclusions and propose a few open problems.

2 | PROBLEM SETTING AND DISCRETIZATION

Consider the following two-dimensional distributed order space-FDE

$$\begin{cases} \frac{\partial u(x,y,t)}{\partial t} = \int_1^2 \left(\frac{\partial^\alpha u(x,y,t)}{\partial |x|^\alpha} + \frac{\partial^\alpha u(x,y,t)}{\partial |y|^\alpha} \right) \rho(\alpha) \mathrm{d}\alpha + f(u,x,y,t), & (x,y,t) \in \Omega \times [0,T], \\ u(x,y,0) = u_0(x,y), & (x,y) \in \Omega, \\ u(x,y,t) = 0, & (x,y) \in \mathbb{R}^2 \setminus \Omega \ \text{ and } \ t \in (0,T], \end{cases} \tag{1}$$

where

$$\Omega = \left\{ (x,y) \in \mathbb{R}^2 \, : \, x \in (\bar{a}, \overline{b}), y \in (c(x), d(x)) \right\} = \left\{ (x,y) \in \mathbb{R}^2 \, : \, y \in (\bar{c}, \overline{d}), x \in (a(y), b(y)) \right\}$$

with

$$\bar{a} := \min a(y), \ \overline{b} := \max b(y), \ \bar{c} := \min c(x), \ \overline{d} := \max d(x)$$

is a convex region, $f(u,x,y,t)$ is the source term, satisfying the Lipschitz condition with respect to u, and $\rho(\alpha)$ is the kernel function satisfying

$$\rho(\alpha) \geq 0, \quad 0 < \int_1^2 \rho(\alpha) \xi(\alpha) \mathrm{d}\alpha < \infty,$$

where $\xi(\alpha) = -\frac{1}{2\cos(\frac{\alpha\pi}{2})} > 0$. The Riesz space fractional derivatives $\frac{\partial^\alpha u(x,y,t)}{\partial |x|^\alpha}$ and $\frac{\partial^\alpha u(x,y,t)}{\partial |y|^\alpha}$ are defined as

$$\begin{aligned} \frac{\partial^\alpha u(x,y,t)}{\partial |x|^\alpha} &= \xi(\alpha) \left({}_{a(y)}D_x^\alpha u(x,y,t) + {}_x D_{b(y)}^\alpha u(x,y,t) \right), \\ \frac{\partial^\alpha u(x,y,t)}{\partial |y|^\alpha} &= \xi(\alpha) \left({}_{c(x)}D_y^\alpha u(x,y,t) + {}_y D_{d(x)}^\alpha u(x,y,t) \right). \end{aligned}$$

Here the left-sided and right-sided Riemann–Liouville fractional derivative operators with respect to x and y are defined as

$$\begin{aligned} {}_{a(y)}D_x^\alpha u(x,y,t) &= \frac{1}{\Gamma(2-\alpha)} \frac{d^2}{dx^2} \int_{a(y)}^x (x-s)^{1-\alpha} u(s,y,t) \mathrm{d}s, \\ {}_x D_{b(y)}^\alpha u(x,y,t) &= \frac{1}{\Gamma(2-\alpha)} \frac{d^2}{dx^2} \int_x^{b(y)} (s-x)^{1-\alpha} u(s,y,t) \mathrm{d}s, \\ {}_{c(x)}D_y^\alpha u(x,y,t) &= \frac{1}{\Gamma(2-\alpha)} \frac{d^2}{dy^2} \int_{c(x)}^y (y-s)^{1-\alpha} u(x,s,t) \mathrm{d}s, \\ {}_y D_{d(x)}^\alpha u(x,y,t) &= \frac{1}{\Gamma(2-\alpha)} \frac{d^2}{dy^2} \int_y^{d(x)} (s-y)^{1-\alpha} u(x,s,t) \mathrm{d}s, \end{aligned}$$

respectively, with $\Gamma(\cdot)$ being the Euler gamma function.

In order to seek the numerical solution without resorting to non-Cartesian meshes, we exploit the volume-penalization method.[9] Before discretizing the equations, we extend the domain Ω to a rectangle $\tilde{\Omega} = [\tilde{a}, \tilde{b}] \times [\tilde{c}, \tilde{d}] \supseteq \Omega$ and reformulate the problem as the following one:

$$\begin{cases} \frac{\partial u_\eta(x,y,t)}{\partial t} = \int_1^2 \left(\frac{\partial^\alpha u_\eta(x,y,t)}{\partial |x|^\alpha} + \frac{\partial^\alpha u_\eta(x,y,t)}{\partial |y|^\alpha} \right) \rho(\alpha) d\alpha - \frac{1 - 1_\Omega(x,y)}{\eta} u_\eta(x,y,t) + \tilde{f}(u_\eta, x, y, t), & (x,y,t) \in \tilde{\Omega} \times [0,T], \\ u_\eta(x,y,0) = \tilde{u}_0(x,y), & (x,y) \in \tilde{\Omega}, \\ u_\eta(x,y,t) = 0, & (x,y) \in \mathbb{R}^2 \setminus \tilde{\Omega} \ \text{ and } \ t \in (0,T], \end{cases} \tag{2}$$

where η is the penalty parameter, 1_Ω is the indicator function defined as

$$1_\Omega(x,y) = \begin{cases} 1, & (x,y) \in \Omega, \\ 0, & (x,y) \in \tilde{\Omega} \setminus \Omega, \end{cases}$$

and $\tilde{f}(u_\eta, x, y, t)$, $\tilde{u}_0(x,y)$ are zero extensions for $f(u,x,y,t)$ and $u_0(x,y)$ respectively, meaning that $\tilde{f}(u_\eta, x, y, t) = 0$, $\tilde{u}_0(x,y) = 0$ when $(x,y) \in \tilde{\Omega} \setminus \Omega$. It is expected that as $\eta \to 0^+$, $u_\eta(x,y,t) \to u(x,y,t)$.

Now, as done in the one-dimensional setting,[20] we adopt a second-order finite difference method to discretize the transformed equations (2). Let M, n_1, and n_2 be positive integers and discretize the domain $\tilde{\Omega} \times [0,T]$ with

$$\begin{aligned} x_i &= \tilde{a} + i h_x, & h_x &= \frac{\tilde{b} - \tilde{a}}{n_1 + 1}, & i &= 0, 1, \dots, n_1 + 1, \\ y_j &= \tilde{c} + j h_y, & h_y &= \frac{\tilde{d} - \tilde{c}}{n_2 + 1}, & j &= 0, 1, \dots, n_2 + 1, \\ t_m &= m \Delta t, & \Delta t &= \frac{T}{M}, & m &= 0, 1, \dots, M. \end{aligned}$$

In order to discretize the left and right Riemann–Liouville fractional derivatives in space, we exploit the weighted and shifted Grünwald–Letnikov difference scheme,[21] that is,

$$\begin{aligned} {}_{\tilde{a}}D_x^\alpha u_\eta(x_i, y_j, t) &= \frac{1}{h_x^\alpha} \sum_{q=0}^{i} \omega_q^{(\alpha)} u_\eta(x_{i-q+1}, y_j, t_m) + \mathcal{O}\left(h_x^2\right), \\ {}_x D_{\tilde{b}}^\alpha u_\eta(x_i, y_j, t) &= \frac{1}{h_x^\alpha} \sum_{q=0}^{n_1 - i + 1} \omega_q^{(\alpha)} u_\eta(x_{i+q-1}, y_j, t_m) + \mathcal{O}\left(h_x^2\right), \\ {}_{\tilde{c}}D_y^\alpha u_\eta(x_i, y_j, t) &= \frac{1}{h_y^\alpha} \sum_{q=0}^{j} \omega_q^{(\alpha)} u_\eta(x_i, y_{j-q+1}, t_m) + \mathcal{O}\left(h_y^2\right), \\ {}_y D_{\tilde{d}}^\alpha u_\eta(x_i, y_j, t) &= \frac{1}{h_y^\alpha} \sum_{q=0}^{n_2 - j + 1} \omega_q^{(\alpha)} u_\eta(x_i, y_{j+q-1}, t_m) + \mathcal{O}\left(h_y^2\right), \end{aligned} \tag{3}$$

where

$$\begin{aligned} &\omega_0^{(\alpha)} = \gamma_1(\alpha) g_0^{(\alpha)}, \quad \omega_1^{(\alpha)} = \gamma_1(\alpha) g_1^{(\alpha)} + \gamma_0(\alpha) g_0^{(\alpha)}, \\ &\omega_k^{(\alpha)} = \gamma_1(\alpha) g_k^{(\alpha)} + \gamma_0(\alpha) g_{k-1}^{(\alpha)} + \gamma_{-1}(\alpha) g_{k-2}^{(\alpha)}, \quad k \geq 2, \end{aligned}$$

in which

$$\begin{aligned} &\gamma_1(\alpha) = \frac{\alpha^2 + 3\alpha + 2}{12}, \ \gamma_0(\alpha) = \frac{4 - \alpha^2}{6}, \ \gamma_{-1}(\alpha) = \frac{\alpha^2 - 3\alpha + 2}{12}, \\ &g_0^{(\alpha)} = 1, \ g_{k+1}^{(\alpha)} = \left(1 - \frac{\alpha + 1}{k + 1}\right) g_k^{(\alpha)}, \quad k \geq 0. \end{aligned}$$

Concerning the discretization in time, as done by Fan and Liu,[7] we take $t_{m+\frac{1}{2}} = t_m + \frac{\Delta t}{2}$ and consider the following second order central difference scheme

$$\frac{\partial u_\eta\left(x_i, y_j, t_{m+\frac{1}{2}}\right)}{\partial t} = \frac{u_\eta(x_i, y_j, t_{m+1}) - u_\eta(x_i, y_j, t_m)}{\Delta t} + \mathcal{O}\left(\Delta t^2\right). \tag{4}$$

In order to approximate the integral in (1), we first decompose it on the subintervals arising from a partition of the integral interval $(1, 2)$. Specifically, we divide the interval $(1, 2)$ into l uniform subintervals and denote by $\Delta\alpha$ the length of such subintervals. Then, the mid-point of each subinterval is given by $\alpha_k = 1 + \left(k - \frac{1}{2}\right)\Delta\alpha$, $k = 1, 2, \dots, l$. By using the mid-point quadrature rule, Equation (1) can be written as

$$\begin{aligned}\int_1^2 \left(\frac{\partial^\alpha u_\eta(x,y,t)}{\partial |x|^\alpha} + \frac{\partial^\alpha u_\eta(x,y,t)}{\partial |y|^\alpha}\right)\rho(\alpha)d\alpha &= \sum_{k=1}^{l} \int_{1+(k-1)\Delta\alpha}^{1+k\Delta\alpha} \left(\frac{\partial^\alpha u_\eta(x,y,t)}{\partial |x|^\alpha} + \frac{\partial^\alpha u_\eta(x,y,t)}{\partial |y|^\alpha}\right)\rho(\alpha)d\alpha \\ &= \sum_{k=1}^{l} \left[\frac{\partial^{\alpha_k} u_\eta(x,y,t)}{\partial |x|^{\alpha_k}} + \frac{\partial^{\alpha_k} u_\eta(x,y,t)}{\partial |y|^{\alpha_k}}\right]\rho(\alpha_k)\Delta\alpha + \mathcal{O}(\Delta\alpha^2). \end{aligned} \tag{5}$$

Due to the nature of the nonlinearity, we can avoid employing a two-level iteration with a nonlinear solver and rather work towards the construction of a two-step implicit scheme. We then we exploit the Lipschitz condition on $\tilde{f}(u_\eta, x, y, t)$ with respect to u_η and find a constant C such that

$$\begin{aligned}&\left|\tilde{f}\left(u_\eta(x_i, y_j, t_{m+\frac{1}{2}}), x_i, y_j, t_{m+\frac{1}{2}}\right) - \tilde{f}\left(\frac{3}{2}u_\eta(x_i, y_j, t_m) - \frac{1}{2}u_\eta(x_i, y_j, t_{m-1}), x_i, y_j, t_{m+\frac{1}{2}}\right)\right| \\ &\leq C\left|u_\eta(x_i, y_j, t_{m+\frac{1}{2}}) - \left(\frac{3}{2}u_\eta(x_i, y_j, t_m) - \frac{1}{2}u_\eta(x_i, y_j, t_{m-1})\right)\right|.\end{aligned}$$

With the additional hypothesis that the second derivative of u_η remains bounded, from Taylor expansions in t_m and t_{m-1} we get

$$\begin{aligned}u_\eta\left(x_i, y_j, t_{m+\frac{1}{2}}\right) &= \frac{3}{2}u_\eta(x_i, y_j, t_{m+\frac{1}{2}}) - \frac{1}{2}u_\eta(x_i, y_j, t_{m+\frac{1}{2}}) \\ &= \frac{3}{2}\left(u_\eta(x_i, y_j, t_m) + \frac{\Delta t}{2}u'_\eta(x_i, y_j, t_m) + \mathcal{O}(\Delta t^2)\right) - \frac{1}{2}\left(u_\eta(x_i, y_j, t_{m-1}) + \frac{3\Delta t}{2}u'_\eta(x_i, y_j, t_{m-1}) + \mathcal{O}(\Delta t^2)\right) \\ &= \frac{3}{2}u_\eta(x_i, y_j, t_m) - \frac{1}{2}u_\eta(x_i, y_j, t_{m-1}) + \frac{3\Delta t}{4}\left(u'_\eta(x_i, y_j, t_m) - u'_\eta(x_i, y_j, t_{m-1}) + \mathcal{O}(\Delta t^2)\right).\end{aligned}$$

From backward and forward finite differences formulas

$$\begin{aligned}u'_\eta(x_i, y_j, t_m) &= \frac{u_\eta(x_i, y_j, t_m) - u_\eta(x_i, y_j, t_{m-1})}{\Delta t} + \mathcal{O}(\Delta t), \\ u'_\eta(x_i, y_j, t_{m-1}) &= \frac{u_\eta(x_i, y_j, t_m) - u_\eta(x_i, y_j, t_{m-1})}{\Delta t} + \mathcal{O}(\Delta t),\end{aligned}$$

therefore

$$u'_\eta(x_i, y_j, t_m) - u'_\eta(x_i, y_j, t_{m-1}) = \mathcal{O}(\Delta t).$$

It follows that

$$u_\eta\left(x_i, y_j, t_{m+\frac{1}{2}}\right) = \frac{3}{2}u_\eta(x_i, y_j, t_m) - \frac{1}{2}u_\eta(x_i, y_j, t_{m-1}) + \mathcal{O}(\Delta t^2),$$

which, combined with the inequality above, provides the following second-order approximation for the nonlinear term at each time step

$$\tilde{f}\left(u_\eta(x_i, y_j, t_{m+\frac{1}{2}}), x_i, y_j, t_{m+\frac{1}{2}}\right) = \tilde{f}\left(\frac{3}{2}u_\eta(x_i, y_j, t_m) - \frac{1}{2}u_\eta(x_i, y_j, t_{m-1}), x_i, y_j, t_{m+\frac{1}{2}}\right) + \mathcal{O}(\Delta t^2). \tag{6}$$

Note that this formula requires the knowledge of $u_\eta(x_i, y_j, t_m)$ and $u_\eta(x_i, y_j, t_{m-1})$, which means that we need to calculate the solution at the first time step in order to start the computation. For this purpose, we will apply one step of the explicit midpoint method

$$u_\eta(x_i, y_j, t_1) = u_\eta(x_i, y_j, t_0) + \Delta t F\left(u_\eta(x_i, y_j, t_0) + \frac{\Delta t}{2}F(u_\eta(x_i, y_j, t_0), x_i, y_j, t_0), x_i, y_j, t_{\frac{1}{2}}\right),$$

where

$$F\big(u_\eta(x,y,t),x,y,t\big) = \int_1^2 \left(\frac{\partial^\alpha u_\eta(x,y,t)}{\partial|x|^\alpha} + \frac{\partial^\alpha u_\eta(x,y,t)}{\partial|y|^\alpha}\right)\rho(\alpha)d\alpha - \frac{1-1_\Omega(x,y)}{\eta}u_\eta(x,y,t) + \tilde{f}(u_\eta(x,y,t),x,y,t).$$

Combining (2)–(6), we obtain

$$\begin{aligned}\frac{u_\eta(x_i,y_j,t_{m+1})-u_\eta(x_i,y_j,t_m)}{\Delta t} &= \Delta\alpha\sum_{k=1}^{l}\frac{\rho(\alpha_k)\xi(\alpha_k)}{h_x^{\alpha_k}}\left(\sum_{q=0}^{i}\omega_q^{(\alpha_k)}u_\eta\left(x_{i-q+1},y_j,t_{m+\frac{1}{2}}\right)+\sum_{q=0}^{n_1-i+1}\omega_q^{(\alpha_k)}u_\eta\left(x_{i+q-1},y_j,t_{m+\frac{1}{2}}\right)\right)\\ &+\Delta\alpha\sum_{k=1}^{l}\frac{\rho(\alpha_k)\xi(\alpha_k)}{h_y^{\alpha_k}}\left(\sum_{q=0}^{j}\omega_q^{(\alpha_k)}u_\eta\left(x_i,y_{j-q+1},t_{m+\frac{1}{2}}\right)+\sum_{q=0}^{n_2-j+1}\omega_q^{(\alpha_k)}u_\eta\left(x_i,y_{j+q-1},t_{m+\frac{1}{2}}\right)\right)\\ &-\frac{1-1_\Omega(x_i,y_j)}{\eta}u_\eta\left(x_i,y_j,t_{m+\frac{1}{2}}\right)+\tilde{f}\left(\frac{3}{2}u_\eta(x_i,y_j,t_m)-\frac{1}{2}u_\eta(x_i,y_j,t_{m-1}),x_i,y_j,t_{m+\frac{1}{2}}\right)+R_{i,j}^m,\end{aligned} \tag{7}$$

where $R_{i,j}^m = \mathcal{O}\big(h_x^2+h_y^2+(\Delta\alpha)^2+(\Delta t)^2\big)$, $1\le i\le n_1$, $1\le j\le n_2$, $1\le m\le M$.

We define the penalization coefficients as

$$d_{i,j} = \begin{cases} 0, & (x_i,y_j)\in\Omega,\\ \frac{\Delta t}{2\eta}, & (x_i,y_j)\in\tilde{\Omega}\setminus\Omega,\end{cases}$$

and denote $\tilde{u}_{i,j}^m \approx u_\eta(x_i,y_j,t_m)$ and $\tilde{f}_{i,j}^m = \tilde{f}\left(\frac{3}{2}u_\eta(x_i,y_j,t_m)-\frac{1}{2}u_\eta(x_i,y_j,t_{m-1}),x_i,y_j,t_{m+\frac{1}{2}}\right)$. By omitting the small terms $R_{i,j}^m$ in (7), we arrive at the following finite difference scheme for solving (2)

$$\begin{aligned}\tilde{u}_{i,j}^{m+1} = \tilde{u}_{i,j}^m &+ \frac{\Delta t\Delta\alpha}{2}\sum_{k=1}^{l}\frac{\rho(\alpha_k)\xi(\alpha_k)}{h_x^{\alpha_k}}\left(\sum_{q=0}^{i}\omega_q^{(\alpha_k)}\left(\tilde{u}_{i-q+1,j}^{m+1}+\tilde{u}_{i-q+1,j}^m\right)+\sum_{q=0}^{n_1-i+1}\omega_q^{(\alpha_k)}\left(\tilde{u}_{i+q-1,j}^{m+1}+\tilde{u}_{i+q-1,j}^m\right)\right)\\ &+\frac{\Delta t\Delta\alpha}{2}\sum_{k=1}^{l}\frac{\rho(\alpha_k)\xi(\alpha_k)}{h_y^{\alpha_k}}\left(\sum_{q=0}^{j}\omega_q^{(\alpha_k)}\left(\tilde{u}_{i,j-q+1}^{m+1}+\tilde{u}_{i,j-q+1}^m\right)+\sum_{q=0}^{n_2-j+1}\omega_q^{(\alpha_k)}\left(\tilde{u}_{i,j+q-1}^{m+1}+\tilde{u}_{i,j+q-1}^m\right)\right)\\ &-d_{i,j}\left(\tilde{u}_{i,j}^{m+1}+\tilde{u}_{i,j}^m\right)+\Delta t\tilde{f}_{i,j}^m,\end{aligned} \tag{8}$$

with the initial condition $\tilde{u}_{i,j}^0 = \tilde{u}_0(x_i,y_j)$, for $i=0,1,\ \dots\ ,n_1+1$, $j=0,1,\ \dots\ ,n_2+1$ and the boundary conditions $\tilde{u}_{i,0}^m = \tilde{u}_{0,j}^m = \tilde{u}_{n_1+1,j}^m = \tilde{u}_{i,n_2+1}^m = 0$ for $m=0,1,\ \dots\ ,M$.

Now, let $N=n_1n_2$, let I_N be the identity of size N, and define

$$\begin{aligned}\tilde{u}^m &= \left[\tilde{u}_{1,1}^m,\ \dots\ ,\tilde{u}_{n_1,1}^m,\tilde{u}_{1,2}^m,\ \dots\ ,\tilde{u}_{n_1,2}^m,\ \dots\ ,\tilde{u}_{1,n_2}^m,\ \dots\ ,\tilde{u}_{n_1,n_2}^m\right]^T,\\ \tilde{f}^m &= \left[\tilde{f}_{1,1}^m,\ \dots\ ,\tilde{f}_{n_1,1}^m,\tilde{f}_{1,2}^m,\ \dots\ ,\tilde{f}_{n_1,2}^m,\ \dots\ ,\tilde{f}_{1,n_2}^m,\ \dots\ ,\tilde{f}_{n_1,n_2}^m\right]^T,\\ D_N &= \operatorname{diag}\left(d_{1,1},\ \dots\ ,d_{n_1,1},d_{1,2},\ \dots\ ,d_{n_1,2},\ \dots\ ,d_{1,n_2},\ \dots\ ,d_{n_1,n_2}\right).\end{aligned}$$

Thus the above numerical scheme (8) can be written in the following matrix form

$$\left(I_N - A_N^x - A_N^y + D_N\right)\tilde{u}^{m+1} = \left(I_N + A_N^x + A_N^y - D_N\right)\tilde{u}^m + \Delta t\tilde{f}^m, \tag{9}$$

with

$$A_N^x = I_{n_2}\otimes\left(\frac{\Delta t\Delta\alpha}{2}\sum_{k=1}^{l}\frac{\rho(\alpha_k)\xi(\alpha_k)}{h_x^{\alpha_k}}A_{n_1}(\alpha_k)\right) =:\ I_{n_2}\otimes B_{n_1}^x, \tag{10}$$

and

$$A_N^y = \left(\frac{\Delta t \Delta \alpha}{2} \sum_{k=1}^{l} \frac{\rho(\alpha_k)\xi(\alpha_k)}{h_y^{\alpha_k}} A_{n_2}(\alpha_k) \right) \otimes I_{n_1} =: B_{n_2}^y \otimes I_{n_1}, \tag{11}$$

where $\otimes$ denotes the usual Kronecker product and

$$A_n(\alpha_k) = \begin{bmatrix} 2\omega_1^{(\alpha_k)} & \omega_0^{(\alpha_k)} + \omega_2^{(\alpha_k)} & \omega_3^{(\alpha_k)} & \cdots & \omega_{n-1}^{(\alpha_k)} & \omega_n^{(\alpha_k)} \\ \omega_0^{(\alpha_k)} + \omega_2^{(\alpha_k)} & 2\omega_1^{(\alpha_k)} & \omega_0^{(\alpha_k)} + \omega_2^{(\alpha_k)} & \omega_3^{(\alpha_k)} & \cdots & \omega_{n-1}^{(\alpha_k)} \\ \vdots & \omega_0^{(\alpha_k)} + \omega_2^{(\alpha_k)} & 2\omega_1^{(\alpha_k)} & \ddots & \ddots & \vdots \\ \vdots & \ddots & \ddots & \ddots & \ddots & \omega_3^{(\alpha_k)} \\ \omega_{n-1}^{(\alpha_k)} & \ddots & \ddots & \ddots & 2\omega_1^{(\alpha_k)} & \omega_0^{(\alpha_k)} + \omega_2^{(\alpha_k)} \\ \omega_n^{(\alpha_k)} & \omega_{n-1}^{(\alpha_k)} & \cdots & \cdots & \omega_0^{(\alpha_k)} + \omega_2^{(\alpha_k)} & 2\omega_1^{(\alpha_k)} \end{bmatrix}.$$

We can also write $A_n(\alpha_k) = A_{\alpha_k,n} + A_{\alpha_k,n}^T$, where

$$A_{\alpha_k,n} = \begin{bmatrix} \omega_1^{(\alpha_k)} & \omega_0^{(\alpha_k)} & 0 & \cdots & 0 & 0 \\ \omega_2^{(\alpha_k)} & \omega_1^{(\alpha_k)} & \omega_0^{(\alpha_k)} & \ddots & \ddots & 0 \\ \vdots & \omega_2^{(\alpha_k)} & \omega_1^{(\alpha_k)} & \ddots & \ddots & \vdots \\ \vdots & \ddots & \ddots & \ddots & \ddots & \vdots \\ \omega_{n-1}^{(\alpha_k)} & \ddots & \ddots & \ddots & \omega_1^{(\alpha_k)} & \omega_0^{(\alpha_k)} \\ \omega_n^{(\alpha_k)} & \omega_{n-1}^{(\alpha_k)} & \cdots & \cdots & \omega_2^{(\alpha_k)} & \omega_1^{(\alpha_k)} \end{bmatrix}.$$

For convenience, we rewrite the linear system in (9) as

$$M_N \tilde{u}^{m+1} = b^m, \tag{12}$$

where

$$M_N = L_N + D_N, \quad L_N = I_N - A_N^x - A_N^y, \quad b^m = \left(I_N + A_N^x + A_N^y - D_N\right)\tilde{u}^m + \Delta t \tilde{f}^m.$$

We stress that as $A_n(\alpha_k)$ is a symmetric Toeplitz matrix, the matrices A_N^x and A_N^y possess a symmetric Block-Toeplitz with Toeplitz-Blocks (BTTB) structure or, in a more precise terminology (see Definition 1), they are 2-level Toeplitz matrices. Since the matrices A_N^x and A_N^y are negative definite,[22] M_N is symmetric positive definite.

3 | SPECTRAL ANALYSIS OF THE COEFFICIENT MATRICES

In this section, we first introduce some basic definitions and results (Section 3.1) and then perform a spectral analysis of the (properly scaled) coefficient matrix-sequence $\{M_N\}_N$ (Section 3.2).

3.1 | Preliminaries

Definition 1. Let $f \in L^1([-\pi,\pi]^d)$ and let $\{f_k\}_{k\in\mathbb{Z}^d}$ be the sequence of its Fourier coefficients defined as

$$f_k := \frac{1}{(2\pi)^d} \int_{[-\pi,\pi]^d} f(\theta) e^{-\mathrm{i}<k,\theta>}\, d\theta,$$

where $< k, \theta >= \sum_{t=1}^{d} k_t \theta_t$. Then the d-level Toeplitz matrix of partial orders $(n_1, n_2, \dots, n_d)$ associated with f is

$$T_N^{(d)} := \left[\cdots \left[\left[f_{i_1-j_1}, f_{i_2-j_2}, \dots, f_{i_d-j_d} \right]_{i_d, j_d=1}^{n_d} \right]_{i_{d-1}, j_{d-1}=1}^{n_{d-1}} \cdots \right]_{i_1, j_1=1}^{n_1},$$

where $N = \Pi_{i=1}^{d} n_i$ is the order of the matrix. The function f is called generating function of the matrix-sequence $\{T_N^{(d)}(f)\}_N$.

To clarify the notation for the case $d = 2$ of interest, the BTTB matrix of order N associated with f is

$$T_N^{(2)}(f) = \left[\left[f_{i_1-j_1}, f_{i_2-j_2} \right]_{i_1, j_1=1}^{n_1} \right]_{i_2, j_2=1}^{n_2},$$

or equivalently,

$$T_N^{(2)}(f) = \sum_{|j_1| \leq n_1} \sum_{|j_2| \leq n_2} f_{j_1, j_2} J_{n_1}^{[j_1]} \otimes J_{n_2}^{[j_2]},$$

where $J_{n_i}^{[j_i]} \in \mathbb{R}^{n_i \times n_i}$, $i = 1, 2$, are matrices whose entry (s, t)th equal 1 if $s - t = j_i$ and is 0 elsewhere.

When $d = 1$, that is, for Toeplitz matrices, we simplify the notation using $T_N(f) := T_N^{(1)}(f)$.

Definition 2. The Wiener class is the set of functions $f(\theta) = \sum_{k \in \mathbb{Z}^d} f_k e^{\mathrm{i} < k, \theta >}$ such that $\sum_{k \in \mathbb{Z}^d} |f_k| < \infty$. The Wiener class forms a sub-algebra of the continuous 2π-periodic functions defined on $[-\pi, \pi]^d$.

We continue giving the definition of the spectral distribution in the sense of the eigenvalues.

Definition 3. Let $f : G \to \mathbb{C}$ be a Lebesgue measurable function, defined on $G \subset \mathbb{R}^k$ with $k \geq 1, 0 < m_k(G) < \infty$, $m_k(\cdot)$ being the Lebesgue measure over $\mathbb{R}^k$. Let $C_0(\mathbb{C})$ be the set of continuous functions with compact support over $\mathbb{C}$ and let $\{\mathcal{A}_N\}_N$ be a sequence of matrices of size N with eigenvalues $\lambda_j(\mathcal{A}_N), j = 1, \dots, N$. We say that $\{\mathcal{A}_N\}_N$ is distributed as the pair (f, G) in the sense of the eigenvalues, and we write

$$\{\mathcal{A}_N\}_N \sim_\lambda (f, G),$$

if the following limit relation holds for all $F \in C_0(\mathbb{C})$:

$$\lim_{N \to \infty} \frac{1}{N} \sum_{j=1}^{N} F(\lambda_j(\mathcal{A}_N)) = \frac{1}{m_k(G)} \int_G F(f(t)) dt.$$

The function f is referred to as the (spectral) symbol.

When $\{\mathcal{A}_N\}_N$ is such that $\{\mathcal{A}_N^* \mathcal{A}_N\}_N \sim_\lambda (0, G)$ for a given G of positive and finite Lebesgue measure, we say that $\{\mathcal{A}_N\}_N$ is a zero-distributed matrix-sequence.

For Hermitian d-level Toeplitz matrix-sequences, the following theorem due to Szegő, Tyrtyshnikov, Tilli, Zamarashkin holds.[23,24]

Theorem 1. *Let $f \in L^1([-\pi, \pi]^d)$ be a real-valued function, then*

$$\left\{ T_N^{(d)}(f) \right\}_N \sim_\lambda (f, [-\pi, \pi]^d).$$

In case of diagonal matrices generated by the characteristic function of a Lebesgue measurable set the following proposition can be proved.[25]

Proposition 1. *Given a Lebesgue measurable set $\Theta \subset [0, 1]^2$ such that the Lebesgue measure of the boundary is 0 and defined the matrix $\mathcal{D}_N(1_\Theta) := \mathrm{diag}_{i=1,\dots,n_1, j=1,\dots,n_2} \left(1_\Theta \left(\frac{i}{n_1+1}, \frac{j}{n_2+1} \right) \right)$, it holds*

$$\{\mathcal{D}_N(1_\Theta)\}_N \sim_\lambda 1_\Theta.$$

With reference to the previous result, notice that a Lebesgue measurable set $\Theta \subset [0,1]^2$, whose boundary Lebesgue measure is 0, is a Peano-Jordan measurable set and vice-versa, so that 1_Θ is a Riemann integrable function. The specification is needed since the two different characterizations and terminologies are used in the literature.[25,26]

We concisely recall that Toeplitz sequences with L^1 symbols, diagonal sampling matrices with Riemann integrable symbols, zero-distributed matrix-sequences (see Definition 3) belong to the generalized locally Toeplitz (GLT) class, which represents a $*$-algebra of matrix-sequences equipped with a symbol that is closed under linear combinations, product, (pseudo) inversion when the symbol is nonzero almost everywhere. The GLT symbol is the spectral symbol in the sense of Definition 3 whenever the considered matrix-sequence is Hermitian or asymptotically Hermitian, where with the term "asymptotically Hermitian" we mean a sequence $\{X_n\}_n$ such that

$$X_n = \Re(X_n) + \mathrm{i}\Im(X_n), \qquad \Re(X_n) = \frac{X_n + X_n^H}{2},\ \Im(X_n) = \frac{X_n - X_n^H}{2},$$

and it exists $p \in [0,\infty]$ such that

$$\lim_{n\to\infty} \frac{\|\Im(X_n)\|_{S,p}}{n^{\frac{1}{p}}} = 0,$$

with $\|\cdot\|_{S,p}$ the Schatten p norm. Without digging deeper into the theory[14] and the general setting,[27] here we only mention that an example of asymptotically Hermitian character is reported in the assumptions of Theorem 2.

We end this introductory part by recalling a property of the spectral norm of d-level Toeplitz matrices and stating a relevant theorem.[27]

Given a square matrix X of order N, we denote its spectral norm by $\|X\|$ that is its maximal singular value ($\|X\| = \max_{i=1,\dots,N} \sigma_i(X)$), which coincides with the spectral radius in the case of a normal matrix and we recall that every Hermitian matrix is also normal. Given a d-level Toeplitz sequence $\{T_N^{(d)}(f)\}_N$ generated by f, it holds that[28]:

$$f \in L^\infty(-\pi,\pi]^d \Rightarrow \|T_N^{(d)}(f)\| \le \|f\|_\infty, \quad \forall N \in \mathbb{N}. \tag{13}$$

Theorem 2 (Corollary 2.8[27]). *Let $\{\mathcal{A}_N\}_N$ be a matrix-sequence with $\mathcal{A}_N = B_N + C_N$ and B_N Hermitian $\forall N \in \mathbb{N}$. Assume that*

- $\{B_N\}_N \sim_\lambda (f,G)$,
- $\|C_N\| = o(1)$.

Then $\{\mathcal{A}_N\}_N \sim_\lambda (f,G)$.

3.2 | Spectral analysis

We are now ready to determine the symbol of our coefficient matrix-sequence. In this view, we start reporting the symbol associated to $\{A_{\alpha_k,n}\}_n$ and to $\{A_n(\alpha_k)\}_n$.[15]

Proposition 2 (Proposition 3.8[15]). *Let $\alpha \in (1,2)$. The symbol associated to the matrix-sequence $\{A_{\alpha,n}\}_n$ belongs to the Wiener class and its formal expression is given by*

$$f_\alpha(\theta) = \sum_{k=-1}^{\infty} \omega_{k+1}^{(\alpha)} e^{\mathrm{i}k\theta} = \left[\frac{8 - 2\alpha^2 + (\alpha^2 + 3\alpha + 2)e^{-\mathrm{i}\theta} + (\alpha^2 - 3\alpha + 2)e^{\mathrm{i}\theta}}{12}\right]\left(1 + e^{\mathrm{i}(\theta+\pi)}\right)^\alpha. \tag{14}$$

Corollary 1 (Corollary 3.9[15]). *Let $\alpha \in (1,2)$. The symbol associated to the matrix-sequence $\{A_n(\alpha) = A_{\alpha,n} + A_{\alpha,n}^T\}_n$ belongs to the Wiener class and its formal expression is given by*

$$g_\alpha(\theta) = f_\alpha(\theta) + f_\alpha(-\theta),$$

where f_α is defined as in (14).

Remark 1. Note that $g_\alpha(\theta)$ is a nonpositive function with a single zero at 0 of order α.

Proposition 3 (Corollary 3.11[15]). *Let* $t_s := \frac{h_s^{\alpha_l}}{\Delta t \Delta \alpha}$ *and assume that* $h_s^{\Delta\alpha} = o(1)$ *with* $s = x, y$. *Then,*

$$\left\{t_x B^x_{n_1}\right\}_{n_1} \sim_\lambda \left(c_l \, g_{\alpha_l}(\theta_1), \; [0,\pi]\right),$$
$$\left\{t_y B^y_{n_2}\right\}_{n_2} \sim_\lambda \left(c_l \, g_{\alpha_l}(\theta_2), \; [0,\pi]\right),$$

where $c_l = \frac{\rho(\alpha_l)\xi(\alpha_l)}{2}$.

By exploiting the previous tools and results, we are in position to discuss the eigenvalue distribution of the (properly scaled) coefficient matrix-sequence $\{M_N\}_N$.

Theorem 3. *Let us assume that* $\frac{t_x}{t_y} = \frac{h_x^{\alpha_l}}{h_y^{\alpha_l}} = \mathcal{O}(1)$, $h_x^{\Delta\alpha} = o(1)$, $h_x^{\alpha_l} = o(\Delta t \Delta \alpha)$, *and* $\eta = \mathcal{O}\left(\frac{h_x^{\alpha_l}}{2\Delta\alpha}\right)$. *We have*

$$\{t_x M_N\}_N \sim_\lambda \left(\mathcal{F}_\alpha(x,y,\theta_1,\theta_2), \; \tilde{\Omega} \times [0,\pi]^2\right)$$

with

$$\mathcal{F}_\alpha(x,y,\theta_1,\theta_2) := \begin{cases} \mathcal{F}_\alpha(\theta_1,\theta_2), & (x,y) \in \Omega, \\ \mathcal{F}_\alpha(\theta_1,\theta_2) + \hat{C}_\eta, & (x,y) \in \tilde{\Omega} \setminus \Omega, \end{cases} \tag{15}$$
$$\mathcal{F}_\alpha(\theta_1,\theta_2) := -c_l\left(g_{\alpha_l}(\theta_1) + \frac{t_x}{t_y} g_{\alpha_l}(\theta_2)\right),$$

and $\hat{C}_\eta = \lim_{h_x,\Delta\alpha\to 0} C_\eta(h_x,\Delta\alpha)$, *where* $C_\eta(h_x,\Delta\alpha) := \frac{h_x^{\alpha_l}}{2\Delta\alpha\eta}$.

Proof. Let us start from

$$t_x M_N = t_x I_N - t_x A^x_N - t_x A^y_N + t_x D_N.$$

As $A^x_N = I_{n_2} \otimes B^x_{n_1} = T_{n_2}(1) \otimes B^x_{n_1}$ and $\left\{t_x B^x_{n_1}\right\}_{n_1} \sim_\lambda (c_l g_{\alpha_l}(\theta_1), [0,\pi])$ where $c_l = \frac{\rho(\alpha_l)\xi(\alpha_l)}{2}$, we have

$$\left\{t_x A^x_N\right\}_N \sim_\lambda \left(c_l \, g_{\alpha_l}(\theta_1), \; [0,\pi]\right).$$

On the other hand,

$$t_x A^y_N = h_x^{\alpha_l}\left(\frac{c_1}{h_y^{\alpha_1}} A_{n_2}(\alpha_1) + \cdots + \frac{c_{l-1}}{h_y^{\alpha_{l-1}}} A_{n_2}(\alpha_{l-1}) + \frac{c_l}{h_y^{\alpha_l}} A_{n_2}(\alpha_l)\right) \otimes I_{n_1}, \tag{16}$$

where $c_k = \frac{\rho(\alpha_k)\xi(\alpha_k)}{2}$, $k = 1, \ldots, l$ and since $1 < \alpha_1 < \alpha_2 < \cdots < \alpha_l < 2$, by using the hypothesis $\frac{t_x}{t_y} = \frac{h_x^{\alpha_l}}{h_y^{\alpha_l}} = \mathcal{O}(1)$, and Equation (13), we have $\left\|c_k \frac{h_x^{\alpha_l}}{h_y^{\alpha_k}} A_{n_2}(\alpha_k)\right\| \leq c_k \frac{h_x^{\alpha_l}}{h_y^{\alpha_k}} \|g_{\alpha_k}\|_\infty \to 0$, which by Theorem 2 with $B_N = \frac{t_x}{t_y} c_l A_{n_2}(\alpha_l)$, $C_N = t_x A^y_N - B_N$ means that

$$\left\{t_x A^y_N\right\}_N \sim_\lambda \left(\frac{t_x}{t_y} c_l g_{\alpha_l}(\theta_2), [0,\pi]\right).$$

Now, let us observe that the matrices $\left\{-t_x A^x_N - t_x A^y_N\right\}_N$ are symmetric two-level Toeplitz and that the function

$$\mathcal{F}_\alpha(\theta_1,\theta_2) := -c_l\left(g_{\alpha_l}(\theta_1) + \frac{t_x}{t_y} g_{\alpha_l}(\theta_2)\right)$$

is real nonnegative. Therefore, by Theorem 1 and by hypothesis $\frac{t_x}{t_y} = \frac{h_x^{\alpha_l}}{h_y^{\alpha_l}} = \mathcal{O}(1)$ we deduce that

$$\left\{-t_x A^x_N - t_x A^y_N\right\}_N \sim_\lambda \left(\mathcal{F}_\alpha(\theta_1,\theta_2), [0,\pi]^2\right).$$

Moreover, as $h_x^{\alpha_l} = o(\Delta t \Delta\alpha)$ it holds that $\|t_x I_N\| = o(1)$ hence again by Theorem 2, this time with $B_N = -t_x A_N^x - t_x A_N^y$ and $C_N = t_x I_N$, it holds

$$\left\{t_x L_N = t_x I_N - t_x A_N^x - t_x A_N^y\right\}_N \sim_\lambda (\mathcal{F}_\alpha(\theta_1, \theta_2), [0, \pi]^2).$$

Now, as $t_x M_N = t_x D_N + t_x L_N$ with $L_N = I_N - A_N^x - A_N^y$ and $D_N = \frac{\Delta t}{2\eta}\mathcal{D}_N\left(1_{\tilde{\Omega}\setminus\Omega}\right)$, it holds that $t_x D_N = \frac{t_x \Delta t}{2\eta}\mathcal{D}_N\left(1_{\tilde{\Omega}\setminus\Omega}\right) = \frac{h_x^{\alpha_l}}{2\Delta\alpha\eta}\mathcal{D}_N\left(1_{\tilde{\Omega}\setminus\Omega}\right) = C_\eta(h_x, \Delta\alpha)\mathcal{D}_N\left(1_{\tilde{\Omega}\setminus\Omega}\right)$. Therefore, by Proposition 1, we obtain

$$\{t_x D_N\}_N \sim_\lambda \hat{C}_\eta \; 1_{\tilde{\Omega}\setminus\Omega}.$$

Finally $\{t_x M_N\}_N \sim_\lambda \mathcal{F}_\alpha(\theta_1, \theta_2)$ on Ω, while $\{t_x M_N\}_N \sim_\lambda \mathcal{F}_\alpha(\theta_1, \theta_2) + \hat{C}_\eta$ on $\tilde{\Omega} \setminus \Omega$ which concludes the proof, because diagonal sampling matrix-sequences and two-level Toeplitz matrix-sequences are GLT sequences and the GLT class is a $*$-algebra. ■

Remark 2. We recall that η should tend to zero. From Theorem 3 it is clear that, in order not to spoil the approximation, η should tend to zero in such a way that $\hat{C}_\eta \to \infty$. For instance, $\eta = O(\Delta t)$ is not sufficient as it implies $\hat{C}_\eta = o(1)$ and $\{t_x M_N\}_N \sim_\lambda \mathcal{F}_\alpha(\theta_1, \theta_2)$ on the whole rectangle $\tilde{\Omega}$.

Remark 3. In proving Theorem 3, taking into account the system (12) and its structure one line below, we implicitly handle the distribution of the Toeplitz-plus-diagonal coefficient matrix sequence, by exploiting the $*$-algebra character of the GLT class and by invoking Proposition 1. Other than that, we could rely on simple Toeplitz tools as the reformulation of 1 as 2 is obtained by means of an additive term $\left(\text{i.e., } \frac{1-1_\Omega(x,y)}{\eta}u_\eta(x, y, t)\right)$.

If in place of the volume-penalization method the original problem (1) is extended in a multiplicative way by replacing (1) with

$$\begin{cases} \frac{\partial u(x,y,t)}{\partial t} = \int_1^2 1_\Omega(x, y)\left(\frac{\partial^\alpha u(x,y,t)}{\partial |x|^\alpha} + \frac{\partial^\alpha u(x,y,t)}{\partial |y|^\alpha}\right)\rho(\alpha)d\alpha + 1_\Omega(x, y)f(u, x, y, t), & (x, y, t) \in \tilde{\Omega} \times [0, T], \\ u(x, y, 0) = 1_\Omega(x, y)u_0(x, y), & (x, y) \in \tilde{\Omega}, \\ u(x, y, t) = 0, & (x, y) \in \mathbb{R}^2 \setminus \tilde{\Omega} \;\text{ and }\; t \in (0, T], \end{cases} \tag{17}$$

then the computation of the symbol can still be performed by resorting to the GLT theory. Indeed, the discretization of Equation (17) in matrix form reads as

$$\begin{cases} \mathcal{D}_N(1_\Omega)L_N\mathcal{D}_N(1_\Omega)u^{m+1} = \mathcal{D}_N(1_\Omega)\left(I_N + A_N^x + A_N^y\right)u^m + \Delta t\mathcal{D}_N(1_\Omega)f^m \\ \mathcal{D}_N(1_{\tilde{\Omega}\setminus\Omega})u^{m+1} = 0 \end{cases}$$

with $L_N = I_N - A_N^x - A_N^y$ and A_N^x, A_N^y as in (10) and (11), and it can be easily shown that $\{t_x\mathcal{D}_N(1_\Omega)L_N\mathcal{D}_N(1_\Omega)\}_N \sim_\lambda 1_\Omega(x, y)\mathcal{F}_\alpha(\theta_1, \theta_2)$, by means of the GLT theory. This kind of approach underlies the reduced GLTs, a more sophisticated tool for computing the symbol of the coefficient matrix that corresponds to (1); see Reference 29, pp. 395–399, Section 3.1.4 Reference 26 for the initial proposal and terminology and Reference 25 for a systematic treatment and for a complete development of the theory. Note that the reduced GLTs have recently been exploited to carry on the spectral analysis for some specific immersed methods for differential problems described by classical derivatives in Reference 30.

Remark 4. We stress that the present proposal takes inspiration from Reference 9 and hence we restrict our attention on convex domains, however, while the assumption is of technical importance for proving existence, uniqueness, regularity and for studying the approximation power of the adopted numerical scheme (as it happens in many contexts when treating PDEs or FDEs), the spectral analysis of the original matrix sequences and of the related preconditioning strategies holds in larger generality due to the structure of $*$-algebra of the reduced generalized locally Toeplitz class. As a matter of fact only the Peano-Jordan measurability of the domain is required which is equivalent to the Riemann integrability of its characteristic function that in turn is equivalent to the zero Lebesgue measure of the frontier of the considered domain.[14]

4 | ALGEBRA PRECONDITIONINGS

In this section, we benchmark the performances of several algebra preconditioners used for solving the linear system (12).

Consider the τ-preconditioners $\mathcal{T}(B^x_{n_1})$ and $\mathcal{T}(B^y_{n_2})$ for the Toeplitz matrices $B^x_{n_1}$ and $B^y_{n_2}$ respectively.[31] The first preconditioner we analyze is defined as

$$\mathcal{T}_N = I_N - I_{n_2} \otimes \mathcal{T}(B^x_{n_1}) - \mathcal{T}(B^y_{n_2}) \otimes I_{n_1}.$$

As a term of comparison, we use the Strang-type preconditioner defined in analogy with $\mathcal{T}_N$ as

$$\mathcal{S}_N = I_N - I_{n_2} \otimes \mathcal{S}(B^x_{n_1}) - \mathcal{S}(B^y_{n_2}) \otimes I_{n_1},$$

where $\mathcal{S}(B^x_{n_1})$ and $\mathcal{S}(B^y_{n_2})$ are the Strang preconditioners for the Toeplitz matrices $B^x_{n_1}$ and $B^y_{n_2}$ respectively.

Both aforementioned matrix-algebra preconditionings do not ensure a superlinear convergence in a multidimensional setting.[16,17] However, the τ-preconditioner is a preferable option in the real symmetric setting,[18] especially because of a substantially better matching of the small eigenvalues.[19]

The following theorem presents the symbol of the (scaled) preconditioners sequences.

Theorem 4. *Assume that* $\frac{t_x}{t_y} = \frac{h_x^{\alpha_l}}{h_y^{\alpha_l}} = \mathcal{O}(1)$, $h_x^{\Delta\alpha} = o(1)$, $h_x^{\alpha_l} = o(\Delta t \Delta\alpha)$, *and* $\eta = \mathcal{O}\left(\frac{h_x^{\alpha_l}}{2\Delta\alpha}\right)$. *It holds*

$$\{t_x \mathcal{T}_N\}_N, \{t_x \mathcal{S}_N\}_N \sim_\lambda \left(\mathcal{F}_\alpha(\theta_1, \theta_2),\ \tilde{\Omega} \times [0, \pi]^2\right),$$

where $\mathcal{F}_\alpha(\theta_1, \theta_2)$ *is defined in (15).*

Proof. It is well-known that the matrix sequences $\{t_x \mathcal{T}(B^x_{n_1})\}_{n_1}$, $\{t_y \mathcal{T}(B^y_{n_2})\}_{n_2}$ have spectral distribution equal to $\{t_x B^x_{n_1}\}_{n_1}$, $\{t_y B^y_{n_2}\}_{n_2}$, respectively, simply because the difference with respect to their Toeplitz counterpart is a zero distributed matrix sequence. For the same reason, the same holds for $\{t_x \mathcal{S}(B^x_{n_1})\}_{n_1}$ and $\{t_y \mathcal{S}(B^y_{n_2})\}_{n_2}$. Then, we obtain the thesis by reasoning as in the proof of Theorem 3. ∎

Note that these preconditioners are highly convenient from a computational point of view because they can be diagonalized through fast transforms, namely discrete sine transform (DST) for $\mathcal{T}_N$ and the FFT for $\mathcal{S}_N$, allowing us to perform the inversion and the matrix-vector product in $\mathcal{O}(N \log(N))$ steps.

For this reason, in both $\mathcal{T}_N$ and $\mathcal{S}_N$ the contribution of the penalization matrix D_N is overlooked, since its presence would prevent the use of fast transforms. On the other hand, this could cause poor performances of PCG, as, due to the presence of D_N, the eigenvalues of M_N present a number (as many as the cardinality of the grid points in $\tilde{\Omega} \setminus \Omega$) of large eigenvalues whose magnitude increases when both the mesh width and η decreases. Indeed, η should be chosen in such a way that the reaction regularization term becomes dominating without spoiling the accuracy of the numerical solution, that is, it should opportunely decrease with the mesh width. We then expect that a too small value of η causes an increase in the iteration of PCG (see the numerical results in the next section).

If we take into account the contribution of D_N, we obtain the second group of preconditioning proposals, defined as

$$\mathcal{T}_N^{\text{split}} = \mathcal{T}_N + D_N = I_N - I_{n_2} \otimes \mathcal{T}(B^x_{n_1}) - \mathcal{T}(B^y_{n_2}) \otimes I_{n_1} + D_N,$$
$$\mathcal{S}_N^{\text{split}} = \mathcal{S}_N + D_N = I_N - I_{n_2} \otimes \mathcal{S}(B^x_{n_1}) - \mathcal{S}(B^y_{n_2}) \otimes I_{n_1} + D_N.$$

We refer to these preconditioners as τ and circulant splitting preconditioners, respectively. As we will explain a few lines down, the reason for this name is that they can be recast as a sum of two contributions on a splitting of $\tilde{\Omega}$.

Let us first determine the symbol of the scaled sequences $\{t_x \mathcal{T}_N^{\text{split}}\}_N$, $\{t_x \mathcal{S}_N^{\text{split}}\}_N$.

Theorem 5. *Assume that* $\frac{t_x}{t_y} = \frac{h_x^{\alpha_l}}{h_y^{\alpha_l}} = \mathcal{O}(1)$, $h_x^{\Delta\alpha} = o(1)$, $h_x^{\alpha_l} = o(\Delta t \Delta\alpha)$, *and* $\eta = \mathcal{O}\left(\frac{h_x^{\alpha_l}}{2\Delta\alpha}\right)$. *It holds*

$$\left\{t_x \mathcal{T}_N^{\text{split}}\right\}_N, \left\{t_x \mathcal{S}_N^{\text{split}}\right\}_N \sim_\lambda \left(\mathcal{F}_\alpha(x, y, \theta_1, \theta_2),\ \tilde{\Omega} \times [0, \pi]^2\right),$$

where $\mathcal{F}_\alpha(x, y, \theta_1, \theta_2)$ *is defined in (15).*

Proof. From Theorem 4 we know that $\{t_x\mathcal{T}_N\}_N, \{t_x\mathcal{S}_N\}_N \sim_\lambda (\mathcal{F}_\alpha(\theta_1,\theta_2),[0,\pi]^2)$. Following again the same reasoning as in Theorem 3 we prove the thesis. ■

It is expected that both $\mathcal{T}_N^{\text{split}}$ and $\mathcal{S}_N^{\text{split}}$ provide a better cluster than $\mathcal{T}_N$ and $\mathcal{S}_N$, since the symbol of the (scaled) split preconditioners is equal to the symbol of the (scaled) coefficient matrix M_N and therefore they take care of all the eigenvalues, including the large eigenvalues related to $\hat{C}_\eta$. However, as we mentioned above, diagonalization through fast transform is not possible and the computation of $\left(\mathcal{T}_N^{\text{split}}\right)^{-1}$ and $\left(\mathcal{S}_N^{\text{split}}\right)^{-1}$ would be too expensive.

This obstacle was overcome in the case of a non-distributed problem,[9] where an analogous τ-splitting preconditioner was presented. What follows is the corresponding adaptation to our distributed case. Let us split the matrix $\mathcal{T}_N^{\text{split}}$ in the form

$$\mathcal{T}_N^{\text{split}} = \mathcal{D}_N(1_\Omega)\mathcal{T}_N + \mathcal{D}_N(1_{\tilde{\Omega}\backslash\Omega})\left(\mathcal{T}_N + \frac{\Delta t}{2\eta}I_N\right). \tag{18}$$

Mimicking this splitting, we define

$$\left(\widehat{\mathcal{T}}_N^{\text{split}}\right)^{-1} := \mathcal{D}_N(1_\Omega)(\mathcal{T}_N)^{-1} + \mathcal{D}_N(1_{\tilde{\Omega}\backslash\Omega})\left(\mathcal{T}_N + \frac{\Delta t}{2\eta}I_N\right)^{-1}.$$

Then it becomes possible to resort to the DST again. The respective circulant version is given by

$$\left(\widehat{\mathcal{S}}_N^{\text{split}}\right)^{-1} := \mathcal{D}_N(1_\Omega)(\mathcal{S}_N)^{-1} + \mathcal{D}_N(1_{\tilde{\Omega}\backslash\Omega})\left(\mathcal{S}_N + \frac{\Delta t}{2\eta}I_N\right)^{-1},$$

which can be diagonalized through the FFT. We stress that such inversion requires two more DSTs/FFTs than the inversion of $\mathcal{T}_N$ and $\mathcal{S}_N$. Moreover, $\left(\widehat{\mathcal{S}}_N^{\text{split}}\right)^{-1}$ and $\left(\widehat{\mathcal{S}}_N^{\text{split}}\right)^{-1}$ are non-symmetric, thus GMRES instead of PCG should be used, which could then cause higher CPU times than PCG.

We now compute the symbol of the scaled sequences $\left\{(t_x\widehat{\mathcal{T}}_N^{\text{split}})^{-1}\right\}_N, \left\{(t_x\widehat{\mathcal{S}}_N^{\text{split}})^{-1}\right\}_N$ and prove that, even if the inverse of the split preconditioners is only approximated, the preconditioned sequences $\left\{(\widehat{\mathcal{T}}_N^{\text{split}})^{-1}M_N\right\}_N, \left\{(\widehat{\mathcal{S}}_N^{\text{split}})^{-1}M_N\right\}_N$ are still (weakly) clustered at 1.

Theorem 6. *Assume that* $\frac{t_x}{t_y} = \frac{h_x^{\alpha_l}}{h_y^{\alpha_l}} = \mathcal{O}(1)$, $h_x^{\Delta\alpha} = o(1)$, $h_x^{\alpha_l} = o(\Delta t\Delta\alpha)$, *and* $\eta = \mathcal{O}\left(\frac{h_x^{\alpha_l}}{2\Delta\alpha}\right)$. *It holds*

$$\left\{(t_x\widehat{\mathcal{T}}_N^{\text{split}})^{-1}\right\}_N, \left\{(t_x\widehat{\mathcal{S}}_N^{\text{split}})^{-1}\right\}_N \sim_\lambda \left(1_\Omega\mathcal{F}_\alpha(\theta_1,\theta_2)^{-1} + 1_{\tilde{\Omega}\backslash\Omega}\left(\mathcal{F}_\alpha(\theta_1,\theta_2)+\hat{C}_\eta\right)^{-1},\ \tilde{\Omega}\times[0,\pi]^2\right),$$

where $\mathcal{F}_\alpha(\theta_1,\theta_2)$ *is defined in (15). Moreover,*

$$\left\{(\widehat{\mathcal{T}}_N^{\text{split}})^{-1}M_N\right\}_N, \left\{(\widehat{\mathcal{S}}_N^{\text{split}})^{-1}M_N\right\}_N \sim_\lambda \left(1,\ \tilde{\Omega}\times[0,\pi]^2\right).$$

Proof. All the involved matrix-sequences clearly belong to the GLT class, because they are diagonal sampling matrix-sequences or Toeplitz matrix-sequences, plus zero-distributed matrix-sequences. Therefore we get the spectral symbol of the sequences of interest by exploiting the structure of $*$-algebra of the GLT class.

From Theorem 4 we know that $\{t_x\mathcal{T}_N\}_N, \{t_x\mathcal{S}_N\}_N \sim_\lambda (\mathcal{F}_\alpha(\theta_1,\theta_2),[0,\pi]^2)$ and consequently $\left\{(t_x\mathcal{T}_N)^{-1}\right\}_N, \left\{(t_x\mathcal{S}_N)^{-1}\right\}_N \sim_\lambda (\mathcal{F}_\alpha(\theta_1,\theta_2)^{-1},[0,\pi]^2)$, while from Proposition 1 we get $\{\mathcal{D}_N(1_\Omega)\}_N \sim_\lambda 1_\Omega$ and $\{\mathcal{D}_N(1_{\tilde{\Omega}\backslash\Omega})\}_N \sim_\lambda 1_{\tilde{\Omega}\backslash\Omega}$. Moreover, it holds

$$\left\{t_x\frac{\Delta t}{2\eta}I_N\right\}_N = \left\{\frac{h_x^{\alpha_l}}{2\Delta\alpha\eta}I_N\right\}_N = \{C_\eta(h_x,\Delta\alpha)I_N\}_N \sim_\lambda \hat{C}_\eta,$$

since $\frac{t_x\Delta t}{2\eta} = \frac{h_x^{\alpha_l}}{2\Delta\alpha\eta} = C_\eta(h_x,\Delta\alpha)$ converges to $\hat{C}_\eta$ as h_x and $\Delta\alpha$ tend to zero. Combining the contributions we get the spectral symbol of the whole sequences $\left\{(t_x\widehat{\mathcal{T}}_N^{\text{split}})^{-1}\right\}_N, \left\{(t_x\widehat{\mathcal{S}}_N^{\text{split}})^{-1}\right\}_N$, which is

$$1_\Omega\mathcal{F}_\alpha(\theta_1,\theta_2)^{-1} + 1_{\tilde{\Omega}\backslash\Omega}\left(\mathcal{F}_\alpha(\theta_1,\theta_2)+\hat{C}_\eta\right)^{-1}.$$

Moreover, the spectral distribution of the preconditioned matrix-sequences $\left\{(\widehat{\mathcal{T}}_N^{\text{split}})^{-1}M_N\right\}_N$, $\left\{(\widehat{\mathcal{S}}_N^{\text{split}})^{-1}M_N\right\}_N$ is given by the product of the symbols of $\left\{(t_x\widehat{\mathcal{T}}_N^{\text{split}})^{-1}\right\}_N$, $\left\{(t_x\widehat{\mathcal{S}}_N^{\text{split}})^{-1}\right\}_N$ and $\{t_xM_N\}_N$ respectively, that is,

$$\begin{aligned}
&\left(1_\Omega\mathcal{F}_\alpha(\theta_1,\theta_2)^{-1}+1_{\tilde{\Omega}\setminus\Omega}\left(\mathcal{F}_\alpha(\theta_1,\theta_2)+\hat{C}_\eta\right)^{-1}\right)\left(1_\Omega\mathcal{F}_\alpha(\theta_1,\theta_2)+1_{\tilde{\Omega}\setminus\Omega}\left(\mathcal{F}_\alpha(\theta_1,\theta_2)+\hat{C}_\eta\right)\right)\\
&=(1_\Omega)^2+(1_{\tilde{\Omega}\setminus\Omega})^2+1_\Omega 1_{\tilde{\Omega}\setminus\Omega}\left(\mathcal{F}_\alpha(\theta_1,\theta_2)^{-1}\left(\mathcal{F}_\alpha(\theta_1,\theta_2)+\hat{C}_\eta\right)+\left(\mathcal{F}_\alpha(\theta_1,\theta_2)+\hat{C}_\eta\right)^{-1}\mathcal{F}_\alpha(\theta_1,\theta_2)\right)\\
&=1_\Omega+1_{\tilde{\Omega}\setminus\Omega}=1_{\tilde{\Omega}},
\end{aligned}$$

since $1_\Omega 1_{\tilde{\Omega}\setminus\Omega}$ is clearly zero everywhere. ■

Remark 5. The symbol for $\left\{t_x\mathcal{T}_N^{\text{split}}\right\}_N$, $\left\{t_x\mathcal{S}_N^{\text{split}}\right\}_N$, and $\{t_xM_N\}_N$ can of course be obtained by leveraging the splitting in (18) as well. In particular, for $\{t_xM_N\}_N$ we have

$$M_N=L_N+D_N=\mathcal{D}_N(1_\Omega)L_N+\mathcal{D}_N(1_{\tilde{\Omega}\setminus\Omega})\left(L_N+\frac{\Delta t}{2\eta}I_N\right).$$

In the following section, we provide numerical examples to test and compare the performances of all discussed the preconditioners.

5 | NUMERICAL EXPERIMENTS

In the current section, we present and critically discuss few selected examples, by emphasizing the performances of the proposed preconditioners and the spectral properties of the different matrix-sequences. We propose three examples with increasing level of generality. In Example 1, we consider a linear problem on a square domain. In Example 2, another linear problem, this time defined on a circular domain, is considered. Finally, in Example 3, the problem of Example 2 is modified by adding a nonlinear term.

5.1 | Example 1

We first consider the two-dimensional version[7] of the example presented in the one-dimensional setting.[15] The problem is defined on the square $\Omega=[0,1]\times[0,1]$ as

$$\begin{cases}\frac{\partial u}{\partial t}=\int_1^2\left(\frac{\partial^\alpha u}{\partial|x|^\alpha}+\frac{\partial^\alpha u}{\partial|y|^\alpha}\right)\rho(\alpha)d\alpha+f(x,y,t), & (x,y,t)\in\Omega\times[0,T],\\ u(x,y,0)=u_0(x,y)=x^2(1-x)y^2(1-y)^2, & (x,y)\in\Omega,\\ u(x,y,t)=0, & (x,y)\in\partial\Omega\ \text{ and }\ t\in(0,T],\end{cases}$$

where

$$\rho(\alpha)=-2\Gamma(5-\alpha)\cos\left(\frac{\alpha\pi}{2}\right),$$
$$f(x,y,t)=e^tx^2(1-x)^2y^2(1-y)^2-e^tx^2(1-x)^2\left[R(y)+R(1-y)\right]-e^ty^2(1-y)^2\left[R(x)+R(1-x)\right],$$

in which Γ is the Gamma function and

$$R(r)=\Gamma(5)R_1(r)-2\Gamma(4)R_2(r)+\Gamma(3)R_3(r)$$

with

$$R_1(r)=\frac{1}{\ln r}(r^3-r^2),$$

$$R_2(r)=\frac{1}{\ln r}(3r^2-2r)+\frac{1}{(\ln r)^2}(r-r^2),$$

$$R_3(r)=\frac{1}{\ln r}(6r-2)+\frac{1}{(\ln r)^2}(3-5r)+\frac{2}{(\ln r)^3}(r-1).$$

The exact solution is given by $u(x,y,t) = e^t x^2(1-x)y^2(1-y)^2$ for $(x,y) \in \Omega$.

5.1.1 | Eigenvalue distribution

We start by numerically verifying the eigenvalue distribution of the scaled coefficient matrix-sequence $\{t_x M_N\}_N$, which in this particular case is lacking of the diagonal term D_N and is therefore a Toeplitz sequence with symbol $\mathcal{F}_\alpha(\theta_1, \theta_2)$. In Figure 1, we compare the eigenvalues of $t_x M_N$ with a uniform sampling of the symbol. We fix $l = 2$ and $n_1 = n_2 = 2^4, 2^7$. It is evident that, as n_1 and n_2 increase, the symbol becomes a better approximation of the eigenvalues. Similar results are obtained for $l = 5$ and are shown in Figure 2, although as l increases larger values of n_1, n_2 are needed to observe the asymptotic relation. The reason of this degradation relies in formula (16), since $l - 1$ terms are neglected in the computation of the symbol because their matrix-sequences are zero-distributed.

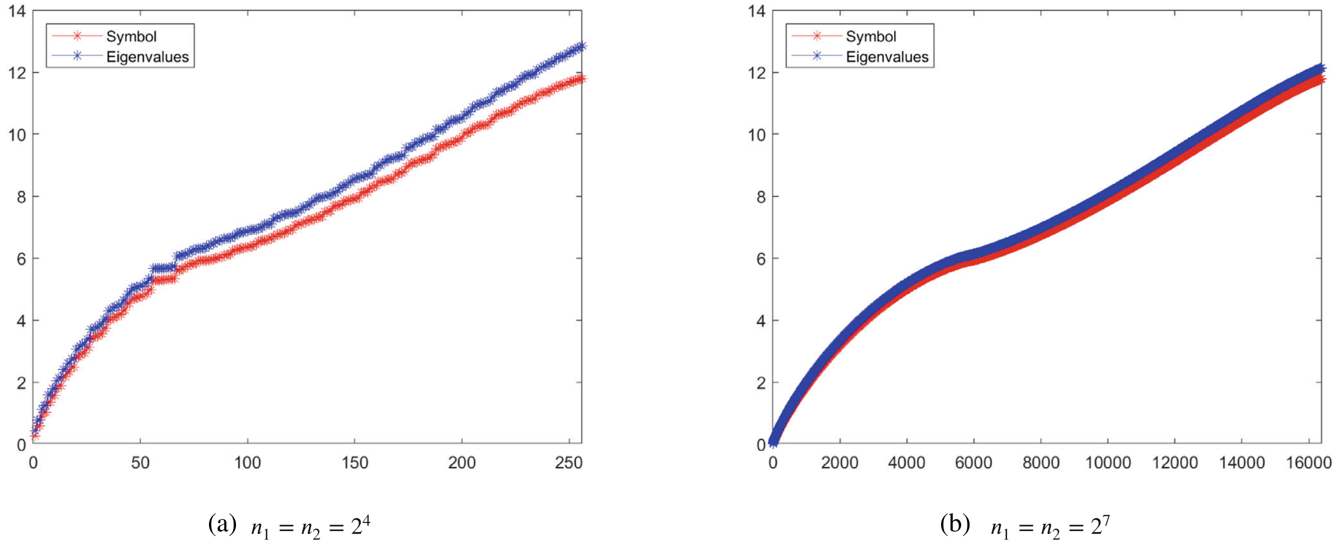

(a) $n_1 = n_2 = 2^4$

(b) $n_1 = n_2 = 2^7$

FIGURE 1 Example 1: Comparison between the symbol $\mathcal{F}_\alpha(\theta_1, \theta_2)$ and eig$(t_x M_N)$ for $l = 2$.

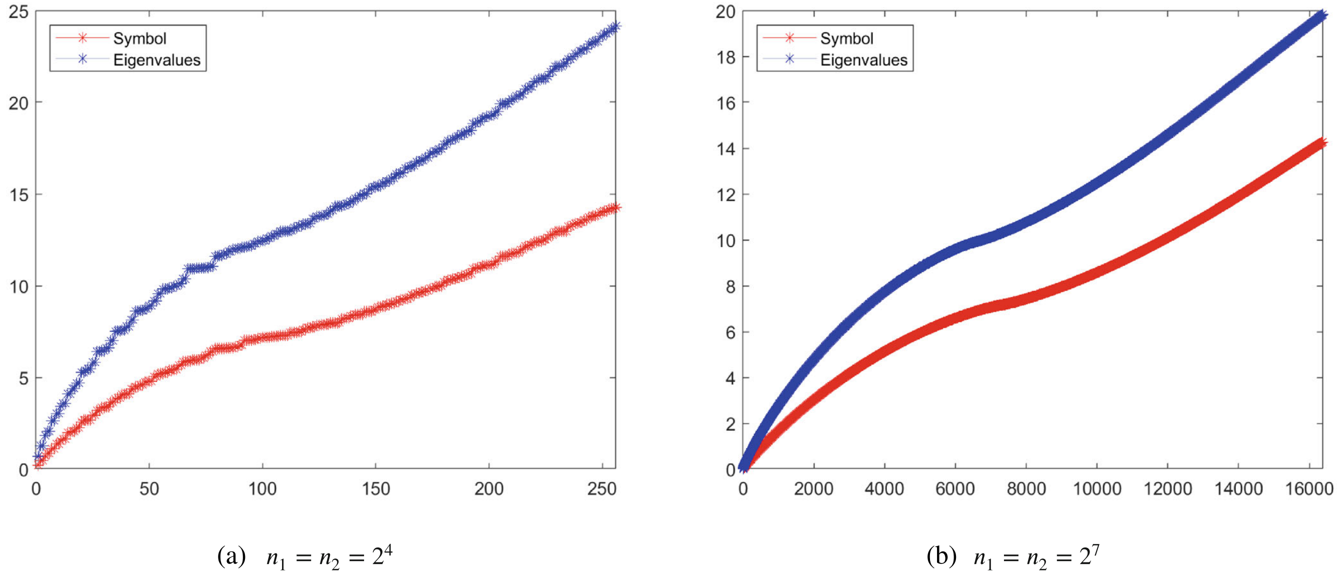

(a) $n_1 = n_2 = 2^4$

(b) $n_1 = n_2 = 2^7$

FIGURE 2 Example 1: Comparison between the symbol $\mathcal{F}_\alpha(\theta_1, \theta_2)$ and eig$(t_x M_N)$ for $l = 5$.

TABLE 1 Example 1: PCG method performances for $\mathcal{S}_N$ and $\mathcal{T}_N$, with tolerance 10^{-8}, $l = 5$, and $\Delta t = 0.1$.

	$\mathcal{S}_N$		$\mathcal{T}_N$	
$n_1 = n_2$	**Iter**	**CPU**	**Iter**	**CPU**
2^4	8.00	0.0027	5.00	0.0027
2^5	9.70	0.0064	5.00	0.0049
2^6	12.10	0.0198	6.00	0.0130
2^7	14.90	0.0598	6.00	0.0367
2^8	18.80	0.3285	6.00	0.1605
2^9	23.20	1.2508	7.00	0.5483
2^{10}	28.60	5.8819	7.00	2.2251

5.1.2 | PCG method

We now discuss the performances of the PCG method. Note that if Ω is a rectangle $\widehat{\mathcal{T}}_N^{\text{split}}$ and $\widehat{\mathcal{S}}_N^{\text{split}}$ coincide with $\mathcal{T}_N$ and $\mathcal{S}_N$, respectively, and for this reason we apply and analyze the PCG method only. In Table 1 the preconditioner $\mathcal{T}_N$ is compared to the circulant one $\mathcal{S}_N$ in terms of iterations and CPU times. We set the tolerance to 10^{-8}, $l = 5$, $n_1 = n_2$, and $\Delta t = 0.1$. "Iter" stands for the average number of iterations at the last time step and "CPU" is the corresponding average CPU timings in seconds.

We note that the τ preconditioner greatly outperforms the circulant one in terms of number of iterations, even for small sizes, and this is reflected in CPU timings, which are smaller for the τ preconditioner. This difference becomes more relevant as n_1, n_2 increase. These results are not unexpected and are consistent with the theoretical predictions in Section 4.

5.2 | Example 2

We now consider a problem defined on a convex region.[7] Let $\Omega = \left\{(x,y) | \frac{x^2}{a^2} + \frac{y^2}{b^2} < 1\right\}$, with $a = b = \frac{1}{4}$, and

$$\begin{cases} \frac{\partial u}{\partial t} = \int_1^2 \left(\frac{\partial^\alpha u}{\partial |x|^\alpha} + \frac{\partial^\alpha u}{\partial |y|^\alpha} \right) \rho(\alpha) d\alpha + f(x,y,t), & (x,y,t) \in \Omega \times [0,T], \\ u(x,y,0) = u_0(x,y) = \left(\frac{x^2}{a^2} + \frac{y^2}{b^2} - 1 \right)^2, & (x,y) \in \Omega, \\ u(x,y,t) = 0, & (x,y) \in \partial\Omega \text{ and } t \in (0,T], \end{cases}$$

where

$$f(x,y,t) = -e^{-t} \left(\frac{x^2}{a^2} + \frac{y^2}{b^2} - 1 \right)^2 - e^{-t} P(x,y,t) - e^{-t} Q(x,y,t),$$

and

$$P(x,y,t) = \frac{\Gamma(5)}{a^4} (R_1(x - x_l) + R_1(x_r - x)) + 4\frac{\Gamma(4)}{a^4} [x_l R_2(x - x_l) - x_r R_2(x_r - x)] + 4\frac{\Gamma(3)}{a^4} \left[x_l^2 R_3(x - x_l) + x_r^2 R_3(x_r - x) \right],$$
$$Q(x,y,t) = \frac{\Gamma(5)}{b^4} (R_1(y - y_l) + R_1(y_r - y)) + 4\frac{\Gamma(4)}{b^4} [y_l R_2(y - y_l) - y_r R_2(y_r - y)] + 4\frac{\Gamma(3)}{b^4} \left[y_l^2 R_3(y - y_l) + y_r^2 R_3(y_r - y) \right],$$

with

$$x_l = -\frac{a}{b} \sqrt{b^2 - y^2}, \qquad x_r = \frac{a}{b} \sqrt{b^2 - y^2},$$

$$y_l = -\frac{b}{a} \sqrt{a^2 - x^2}, \qquad y_r = \frac{b}{a} \sqrt{a^2 - x^2},$$

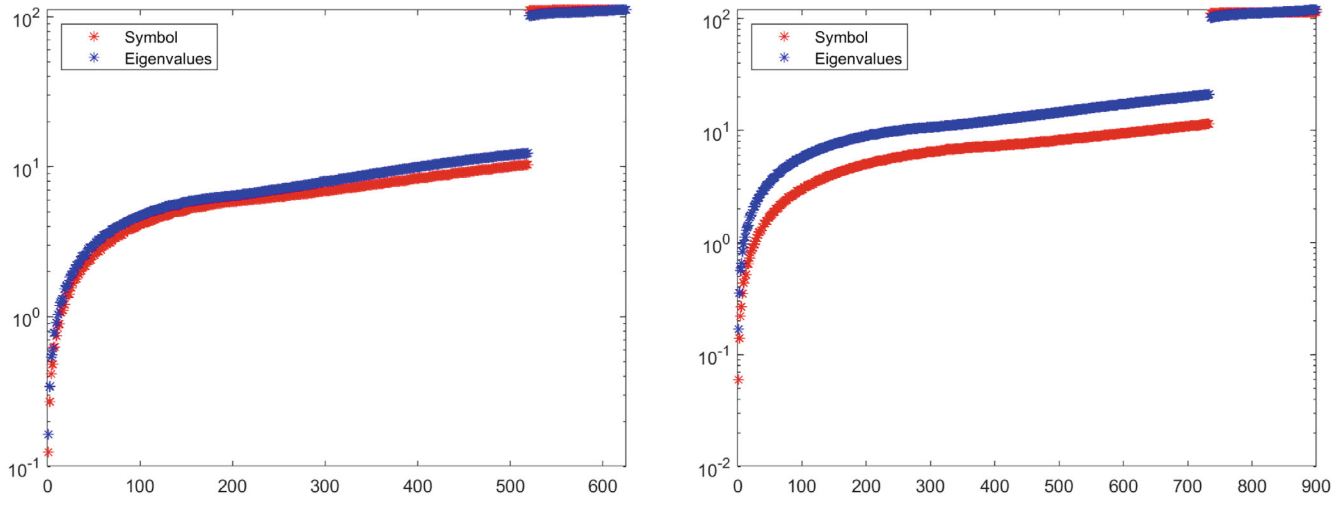

(a) $l = 2$

(b) $l = 5$

FIGURE 3 Example 2: Comparison between the symbol $\mathcal{F}_\alpha(x, y, \theta_1, \theta_2)$ and $\mathrm{eig}(t_x M_N)$ with $\eta = 10^{-5}$ and $C_\eta(h_x, \Delta\alpha) = 100$.

and R_1, R_2, R_3, $\rho(\alpha)$ defined as in Example 1. The exact solution for this problem is $u(x, y, t) = e^{-t}\left(\frac{x^2}{a^2} + \frac{y^2}{b^2} - 1\right)^2$. In the application of the volume-penalization method, we extend the domain Ω to the rectangle $\tilde{\Omega} = [-a, a] \times [-b, b]$.

5.2.1 | Eigenvalue distribution

First, we want to verify the eigenvalue distribution of the scaled coefficient matrices, as portrayed in Theorem 3. In this case, M_N contains the penalization term D_N and therefore the sequence $\{t_x M_N\}_N$ is associated to the symbol $\mathcal{F}_\alpha(x, y, \theta_1, \theta_2)$.

In Figure 3, we compare the eigenvalues of $t_x M_N$ with a uniform sampling of the symbol, setting $\eta = 10^{-5}$ and adjusting h_x and $\Delta\alpha$ to obtain $C_\eta(h_x, \Delta\alpha) = 100$. The symbol provides a reliable approximation of the eigenvalues. We have already noted in Example 1 that as l increases the spectral distribution result still holds asymptotically, but we would need a smaller h_x to observe it, and again as discussed before the reason relies in the nature of formula (16).

Now, in order to observe the behavior as η tends to zero and n_1, n_2 tend to infinity, we vary η and n_1, n_2, maintaining $n_1 = n_2$. We recall that in Theorem 3 we requested that $\eta = \mathcal{O}\left(\frac{h_x^{\alpha_l}}{2\Delta\alpha}\right)$. Having fixed $\Delta\alpha$, this means that n_1 and η should be chosen such that η and $h_x^{\alpha_l}$ balance each other. Figure 4 highlights this fact. When $n_1 = 2^4$, $\eta = 10^{-2}$ is not small enough to counterbalance $h_x^{\alpha_l}$ and, as a consequence, it is not possible to discern the part of the symbol corresponding to the domain Ω and the one corresponding to its complement. In other words, we are not able to identify the solution on the domain of interest. If we decrease η to 10^{-4}, the separation becomes perceptible.

The same happens if we set $n_1 = 2^6$, as shown in Figure 5. For $\eta = 10^{-4}$ there is no distinction between the two portions of the plot, while with the smaller value $\eta = 10^{-6}$ the gap is apparent.

5.2.2 | PCG and GMRES method

Next, we discuss the performance of the PCG and GMRES methods with the proposed preconditioners. The results are shown in Table 2, with tolerance set to 10^{-8}, $l = 5$, $n_1 = n_2$ and $\Delta t = 0.1$.

First, we examine $\widehat{\mathcal{T}}_N^{\text{split}}$, $\mathcal{T}_N$ compared to $\widehat{\mathcal{S}}_N^{\text{split}}$, $\mathcal{S}_N$. As in Example 1, the superior performance of both the τ-preconditioners in relation to their respective circulant counterparts is evident and consistent with theoretical predictions in Section 4.

Nonetheless, we observe that the ratio between the iterations required for $\mathcal{S}_N$ and $\mathcal{T}_N$, or likewise between those required for $\widehat{\mathcal{S}}_N^{\text{split}}$ and $\widehat{\mathcal{T}}_N^{\text{split}}$, is greater than the ratio between the corresponding CPU times. In other words, the difference between the CPU times does not fully reflect the considerable difference in the required iterations. This is due to the fact

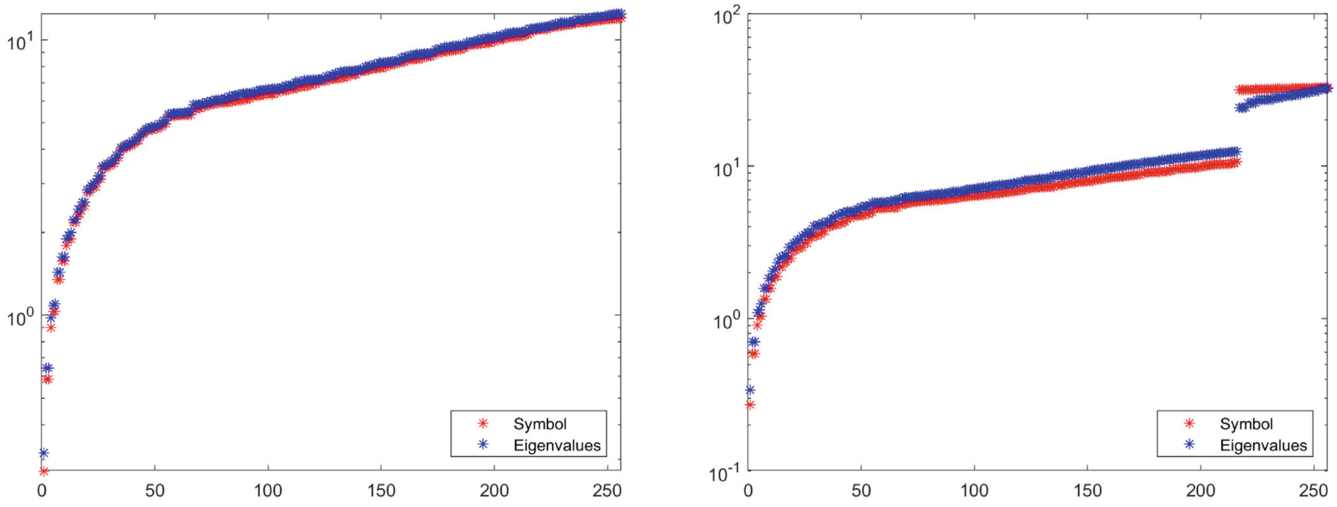

(a) $\eta = 10^{-2}$

(b) $\eta = 10^{-4}$

FIGURE 4 Example 2: Comparison between the symbol $\mathcal{F}_\alpha(x, y, \theta_1, \theta_2)$ and $\mathrm{eig}(t_x M_N)$ with $l = 2$ and $n_1 = n_2 = 2^4$.

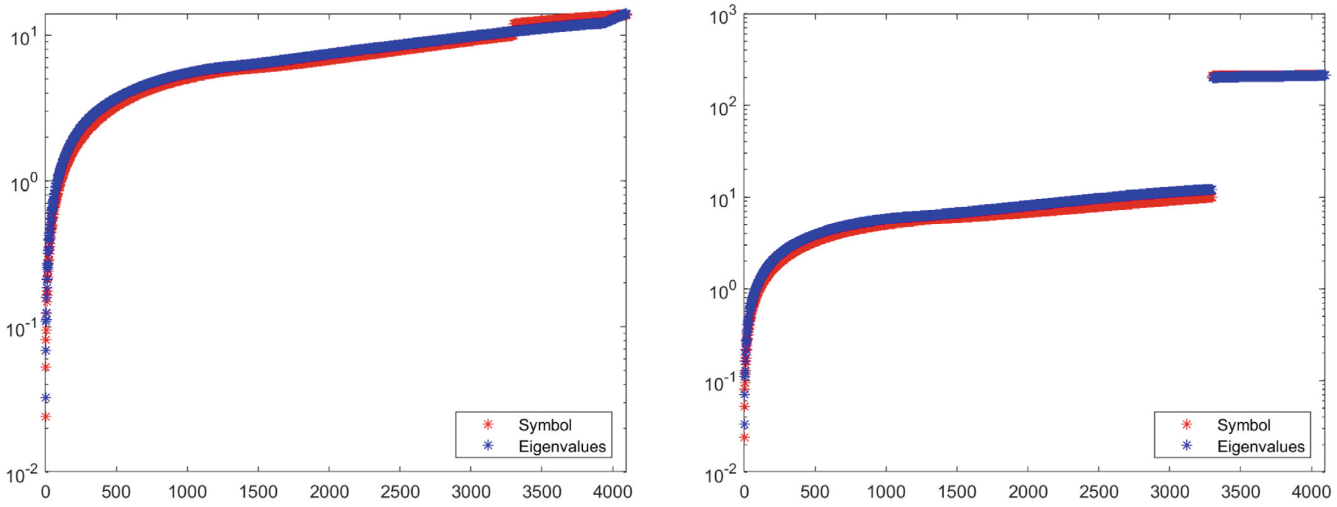

(a) $\eta = 10^{-4}$

(b) $\eta = 10^{-6}$

FIGURE 5 Example 2: Comparison between the symbol $\mathcal{F}_\alpha(x, y, \theta_1, \theta_2)$ and $\mathrm{eig}(t_x M_N)$ with $l = 2$ and $n = 2^6$.

that the circulant preconditioners are implemented by the means of the FFT, while the τ-preconditioners employ the DST, which in MATLAB is implemented via two FFTs. Then, the computation of $\mathcal{T}_N$ in MATLAB requires twice the number of FFTs as compared to $\mathcal{S}_N$, and the same holds for $\hat{\mathcal{T}}_N^{\mathrm{split}}$ and $\hat{\mathcal{S}}_N^{\mathrm{split}}$. The use of an algorithm less computationally expensive for computing the DST would lead to lower CPU times for the τ-preconditioners, especially for smaller sizes. In this direction, for n power of 2, the Van Loan book[32] indicates a floating point cost of the FFT as $4n\log_2(n)$ operations while with the same setting the DST operation count amounts to $\frac{5}{2}n\log_2(n)$ and the same type of advantage in favor of the DST holds for generic sizes. Therefore, with a careful implementation of the DST, we would have a CPU timing substantially in favor of the τ approach, when compared with the circulant one.

Now, let us analyze the performance of $\hat{\mathcal{T}}_N^{\mathrm{split}}, \hat{\mathcal{S}}_N^{\mathrm{split}}$ compared to $\mathcal{T}_N, \mathcal{S}_N$. Since, as shown in Section 4, the symbol of the split preconditioners matches the symbol of the coefficient matrix, contrary to the symbol of the non-split preconditioners which does not include the term arising from the penalty matrix, we expect the split preconditioners to be the favored choice. This is confirmed by the numerical results collected in Table 2, where the number of iterations required by the split preconditioners is lower than their respective non-split versions. The same effect is reflected in the CPU times for small

TABLE 2 Example 2: PCG versus GMRES method performances, with tolerance 10^{-8}, $l = 5$, and $\Delta t = 0.1$.

		PCG				GMRES			
		$\mathcal{S}_N$		$\mathcal{T}_N$		$\widehat{\mathcal{S}}_N^{\text{split}}$		$\widehat{\mathcal{T}}_N^{\text{split}}$	
η	n_1	Iter	CPU	Iter	CPU	Iter	CPU	Iter	CPU
10^{-2}	2^4	10.00	0.0030	6.00	0.0030	8.90	0.0040	5.70	0.0048
	2^5	11.50	0.0071	6.00	0.0055	10.00	0.0088	5.60	0.0085
	2^6	16.50	0.0260	6.00	0.0130	12.80	0.0302	5.60	0.0184
	2^7	19.90	0.0732	6.00	0.0353	16.30	0.0940	5.50	0.0643
	2^8	25.40	0.2678	6.00	0.1093	20.80	0.3351	5.50	0.1936
	2^9	31.60	1.5522	6.40	0.4791	25.50	1.7642	5.20	0.6831
	2^{10}	40.40	7.8513	6.50	2.0485	31.00	8.9884	5.00	3.2243
10^{-3}	2^4	13.50	0.0037	9.30	0.0041	9.00	0.0038	8.00	0.0060
	2^5	14.00	0.0083	8.00	0.0069	11.00	0.0093	7.00	0.0104
	2^6	16.80	0.0264	8.00	0.0166	12.50	0.0305	7.00	0.0225
	2^7	20.60	0.0745	8.00	0.0448	15.00	0.0838	7.00	0.0754
	2^8	27.20	0.2881	8.00	0.1415	18.70	0.2873	7.00	0.2290
	2^9	32.00	1.4874	8.00	0.5578	23.40	1.5383	7.00	0.8259
	2^{10}	42.10	8.5684	8.20	2.5449	30.20	10.8054	7.00	4.9177
10^{-4}	2^4	21.80	0.0065	17.10	0.0079	10.00	0.0063	9.00	0.0109
	2^5	24.40	0.0138	17.40	0.0140	12.00	0.0135	10.70	0.0215
	2^6	25.60	0.0405	16.80	0.0341	13.00	0.0412	10.30	0.0469
	2^7	26.80	0.0962	15.60	0.0813	15.20	0.1296	10.00	0.1460
	2^8	30.40	0.3130	15.30	0.2570	18.50	0.5765	10.00	0.5320
	2^9	37.90	1.8608	15.10	1.0310	22.70	2.6973	10.00	2.0241
	2^{10}	47.30	9.4967	15.10	4.4302	27.00	7.1147	10.00	4.7834
10^{-5}	2^4	26.10	0.0068	25.60	0.0104	10.00	0.0044	9.70	0.0075
	2^5	44.70	0.0249	34.50	0.0271	12.40	0.0103	12.00	0.0159
	2^6	51.60	0.0799	40.30	0.0786	16.00	0.0425	13.60	0.0437
	2^7	56.90	0.2002	39.50	0.2093	18.40	0.1069	14.30	0.1464
	2^8	60.30	0.6293	40.90	0.6737	19.30	0.3068	15.00	0.4474
	2^9	64.50	3.1523	40.70	2.7035	21.70	2.0571	14.40	2.1930
	2^{10}	70.30	14.1906	40.10	11.3976	24.40	7.8825	14.00	7.7301

enough values of the penalization parameter. In fact, as a result of the cost per iteration of the GMRES method and the need of two extra FFTs/DSTs, when the penalization parameter is not sufficiently small, the lower number of iterations provided by the split choice does not translate to equally lower CPU times. For this example we see the advantage of using the split preconditioners when $\eta = 10^{-5}$.

Finally, we observe that the increase in accuracy given by smaller values of η comes at the cost of an increased number of iterations, and that this is more evident for CG with $\mathcal{T}_N$, $\mathcal{S}_N$ preconditioners.

5.2.3 | Error analysis

To conclude, we briefly discuss the error and its relation to the penalization parameter. Table 3 collects the error for several values of $n_1 = n_2$ and η, computed as the l^2 norm of the difference between the exact and the approximated solution. The

TABLE 3 Example 2: PCG versus GMRES method performances, with tolerance 10^{-6}, $l = 10$, and $\Delta t = 0.1$.

	$\eta = 10^{-2}$		$\eta = 10^{-3}$		$\eta = 10^{-4}$		$\eta = 10^{-5}$	
n_1	ErrIn	ErrOut	ErrIn	ErrOut	ErrIn	ErrOut	ErrIn	ErrOut
2^4	4.23e−03	8.10e−04	1.96e−03	1.17e−03	1.33e−03	3.44e−04	1.38e−03	4.15e−05
2^5	1.44e−03	4.35e−04	7.42e−04	5.24e−04	3.89e−04	1.87e−04	4.54e−04	2.57e−05
2^6	1.18e−03	3.97e−04	7.43e−04	4.19e−04	1.88e−04	1.75e−04	7.90e−05	2.74e−05
2^7	7.59e−04	3.18e−04	5.08e−04	3.14e−04	1.49e−04	1.30e−04	9.71e−06	2.18e−05
2^8	6.67e−04	3.22e−04	4.56e−04	3.06e−04	1.42e−04	1.21e−04	1.58e−05	1.98e−05

tolerance is 10^{-6}, $l = 10$ and $\Delta t = 0.1$. The errors obtained with the different methods and preconditioners are all equal, therefore only the one related to $\mathcal{T}_N$ is shown. "ErrIn" designates the error inside the domain Ω, while "ErrOut" indicates the error on $\tilde{\Omega} \setminus \Omega$. The latter coincides with the l^2 norm of the numerical solution on the same set and is also referred to as "penalty error".

- From (7) we know that the truncation error produced by the approximation is $\mathcal{O}\big(h_x^2 + h_y^2 + (\Delta\alpha)^2 + (\Delta t)^2\big)$. With the fixed values $\Delta\alpha = 0.1$ and $\Delta t = 0.1$ selected for the experiments, we do not expect to see a significant improvement in accuracy as n_1, n_2 increase. Nevertheless, the proposed numerical method appears to be precise and reliable.
- Regarding the penalization parameter, we observe that the error slightly improves for smaller values of η. However, as n_1 increases the error ceases to decrease once the order of the penalty error is reached, because the penalty error dominates over the global truncation error. For instance, with $\eta = 10^{-2}$ ErrIn remains of order 10^{-4} at most, following the penalty error ErrOut, and further refinements of the spatial grid cannot improve the accuracy of the numerical solution. Conversely, with $\eta = 10^{-5}$ ErrIn manages to reach the order 10^{-5}, since that is the order of the penalty error.

5.3 | Example 3

For the last example, we modify the problem from the previous example by inserting a nonlinear term

$$\begin{cases} \frac{\partial u}{\partial t} = \int_1^2 \left(\frac{\partial^\alpha u}{\partial |x|^\alpha} + \frac{\partial^\alpha u}{\partial |y|^\alpha} \right) \rho(\alpha) d\alpha + f(u, x, y, t), & (x, y, t) \in \Omega \times [0, T], \\ u(x, y, 0) = u_0(x, y) = \left(\frac{x^2}{a^2} + \frac{y^2}{b^2} - 1 \right)^2, & (x, y) \in \Omega, \\ u(x, y, t) = 0, & (x, y) \in \partial\Omega \text{ and } t \in (0, T], \end{cases}$$

with

$$f(u, x, y, t) = u(x, y, t)(1 - u(x, y, t))$$

on the domain Ω defined above which is once again extended to the rectangle $\tilde{\Omega}$ in the volume-penalization method. Here, the exact solution is not known.

Since the only change made, with respect to Example 2, is in the source term, the coefficient matrix-sequence remains the same and the comparison between the symbol and the eigenvalues would be redundant. Therefore, we move directly to the analysis of the numerical methods. We set the tolerance, l and Δt as in Example 2 and apply the PCG and GMRES methods with their respective preconditioners. The obtained results are gathered in Table 4 and are consistent with the observations made in the previous examples.

TABLE 4 Example 3: PCG versus GMRES method performances, with tolerance 10^{-8}, $l = 5$, and $\Delta t = 0.1$.

		PCG				**GMRES**			
		$\mathcal{S}_N$		$\mathcal{T}_N$		$\hat{\mathcal{S}}_N^{\mathbf{split}}$		$\hat{\mathcal{T}}_N^{\mathbf{split}}$	
$\boldsymbol{\eta}$	$\boldsymbol{n_1}$	**Iter**	**CPU**	**Iter**	**CPU**	**Iter**	**CPU**	**Iter**	**CPU**
10^{-2}	2^4	9.60	0.0032	5.10	0.0028	10.00	0.0051	6.00	0.0057
	2^5	11.10	0.0070	5.10	0.0049	11.80	0.0098	6.10	0.0088
	2^6	15.10	0.0243	5.10	0.0114	14.60	0.0344	6.10	0.0197
	2^7	18.90	0.0708	5.10	0.0313	18.20	0.1001	6.00	0.0640
	2^8	22.90	0.2479	5.10	0.0983	22.60	0.3865	7.00	0.2227
	2^9	29.90	1.9227	5.20	0.4682	27.20	1.9674	7.00	0.8897
	2^{10}	35.50	7.6379	5.80	1.9621	32.80	9.3339	6.20	3.5411
10^{-3}	2^4	12.50	0.0035	9.10	0.0041	10.10	0.0040	8.60	0.0062
	2^5	13.80	0.0083	8.10	0.0071	12.00	0.0097	8.10	0.0109
	2^6	16.70	0.0269	7.10	0.0153	14.80	0.0337	8.00	0.0232
	2^7	19.00	0.0689	7.10	0.0409	17.00	0.0940	8.00	0.0808
	2^8	24.10	0.2527	7.00	0.1242	21.80	0.3503	8.00	0.2581
	2^9	30.10	1.5727	7.00	0.5657	26.90	1.9032	8.00	0.9314
	2^{10}	43.30	8.7480	8.10	2.5431	34.20	9.9982	7.20	3.9584
10^{-4}	2^4	20.20	0.0053	17.10	0.0076	10.90	0.0043	10.00	0.0072
	2^5	22.10	0.0127	16.10	0.0132	13.90	0.0110	12.30	0.0160
	2^6	23.00	0.0356	14.90	0.0294	16.80	0.0399	13.00	0.0365
	2^7	24.60	0.0877	14.00	0.0759	19.20	0.1052	13.00	0.1201
	2^8	27.30	0.2867	13.00	0.2185	22.40	0.3630	13.00	0.3867
	2^9	32.40	1.6974	12.80	0.8859	26.30	1.8314	13.00	1.4260
	2^{10}	40.60	8.4656	12.10	3.6506	30.80	8.5429	12.10	5.8676
10^{-5}	2^4	29.30	0.0075	26.40	0.0107	10.80	0.0043	10.80	0.0074
	2^5	42.90	0.0237	32.20	0.0253	16.00	0.0127	13.90	0.0179
	2^6	48.40	0.0725	36.50	0.0706	21.40	0.0526	16.90	0.0488
	2^7	53.20	0.1872	35.50	0.1922	24.60	0.1363	18.90	0.1713
	2^8	53.10	0.5463	34.90	0.5706	27.80	0.4534	20.90	0.6058
	2^9	54.00	2.7608	34.00	2.2506	28.50	1.9706	21.10	2.1799
	2^{10}	59.10	12.4349	33.10	9.5666	31.50	9.0901	20.70	9.7011

6 | CONCLUSIONS AND OPEN PROBLEMS

In the present paper, we considered the numerical solution of a two-dimensional constant coefficient distributed-order space-FDE, where additional challenges are given by the presence of a nonlinear term and by the domain which is convex but not necessarily Cartesian.

The problem has been reformulated in such a way that a more convenient Cartesian structure of the domain is recovered, by using a proper penalization technique. The resulting linear systems show structured coefficient matrices, which can be indeed represented as the sum of a diagonal (sampling) matrix and a two-level Toeplitz matrix with continuous generating function. The resulting matrix-sequences belong to the class of the GLT sequences and the related spectral analysis has been provided by minimizing the technicalities of the powerful GLT apparatus. Associated fast iterative solvers have been proposed and studied. The related numerical performances have been reported and critically discussed.

As future work, it would be interesting to study the localization of the spectra of the preconditioned matrix-sequences, for fixed dimensions and in terms of the various problem and approximation parameters, in order to check the robustness of the proposed methods: this would allow precise estimates of the convergence speed by using classical and important results, such as those started with the pioneering work by Axelsson and Lindskög.[33]

ACKNOWLEDGMENTS

The authors are members of the Italian INdAM-GNCS group. This work was supported by INdAM-GNCS project CUP E53C22001930001 granted to Mariarosa Mazza. Furthermore, the work of Stefano Serra-Capizzano was funded from the European High-Performance Computing Joint Undertaking (JU) under Grant agreement No. 955701. The JU receives support from the European Union's Horizon 2020 Research and Innovation Program and Belgium, France, Germany, Switzerland. Furthermore Stefano Serra-Capizzano is grateful for the support of the Laboratory of Theory, Economics and Systems - Department of Computer Science at Athens University of Economics and Business.

CONFLICT OF INTEREST STATEMENT

This study does not have any conflicts to disclose.

DATA AVAILABILITY STATEMENT

The data that support the findings of this study are available from the corresponding author upon reasonable request.

ORCID

Rosita Luisa Sormani https://orcid.org/0009-0005-6185-6886

REFERENCES

1. Bagley RL, Torvik PJ. On the existence of the order domain and the solution of distributed order equations—part I. Int J Appl Math. 2000;2(7):865–82.
2. Bagley RL, Torvik PJ. On the existence of the order domain and the solution of distributed order equations—part II. Int J Appl Math. 2000;2(8):965–87.
3. Caputo M. Diffusion with space memory modelled with distributed order space fractional differential equations. Ann Geophys. 2003;46:223–34.
4. Podlubny I. Fractional differential equations: an introduction to fractional derivatives, fractional differential equations, to methods of their solution and some of their applications. Vol 198. Cambridge, MA: Academic Press; 1998.
5. Su NH. Distributed-order infiltration, absorption and water exchange in mobile and immobile zones of swelling soils. J Hydrol. 2012;468-469:1–10.
6. Su NH, Nelson PN, Connor S. The distributed-order fractional diffusion-wave equation of groundwater flow: theory and application to pumping and slug tests. J Hydrol. 2015;529:1262–73.
7. Fan W, Liu F. A numerical method for solving the two-dimensional distributed order space-fractional diffusion equation on an irregular convex domain. Appl Math Lett. 2018;77:114–21.
8. Angot P, Bruneau CH, Fabrie P. A penalization method to take into account obstacles in incompressible viscous flows. Numer Math. 1999;81:497–520.
9. Huang X, Sun HW. A preconditioner based on sine transform for two-dimensional semi-linear Riesz space fractional diffusion equations in convex domains. Appl Numer Math. 2021;169:289–302.
10. Li Z, Ito K. The immersed Interface method: numerical solutions of PDEs involving interfaces and irregular domains. Philadelphia, PA: SIAM; 2006.
11. De Prenter F, Verhoosel CV, Van Brummelen EH, Larson MG, Badia S. Stability and conditioning of immersed finite element methods: analysis and remedies. Arch Comput Methods Eng. 2023;30(6):3617–56.
12. Marchuk GI, Kuznetsov YA, Matsokin AM. Fictitious domain and domain decomposition methods. Sov J Numer Anal Math Model. 1986;1-1:3–35.
13. Glowinski R, Kuznetsov YA. Distributed Lagrange multipliers based on fictitious domain method for second order elliptic problems. Comput Methods Appl Mech Eng. 2007;196-8:1498–506.
14. Garoni C, Serra-Capizzano S. Generalized locally Toeplitz sequences: theory and applications (Vol. II). Cham: Springer; 2018.
15. Mazza M, Serra-Capizzano S, Usman M. Symbol-based preconditioning for Riesz distributed-order space-fractional diffusion equations. Electron Trans Numer Anal. 2021;54:499–513.
16. Serra-Capizzano S, Tyrtyshnikov EE. Any circulant-like preconditioner for multilevel matrices is not superlinear. SIAM J Matrix Anal Appl. 1999;21(2):431–9.
17. Serra-Capizzano S, Tyrtyshnikov EE. How to prove that a preconditioner cannot be superlinear. Math Comput. 2003;72(243):1305–16.
18. Serra-Capizzano S. Toeplitz preconditioners constructed from linear approximation processes. SIAM J Matrix Anal Appl. 1998;20(2):446–65.

19. Barakitis N, Ekström S-E, Vassalos P. Preconditioners for fractional diffusion equations based on the spectral symbol. Numer. Linear Algebra Appl. 2022;29(5):e2441.
20. Abbaszadeh M. Error estimate of second-order finite difference scheme for solving the Riesz space distributed-order diffusion equation. Appl Math Lett. 2019;88:179–85.
21. Hao Z, Sun Z, Cao W. A fourth-order approximation of fractional derivatives with its applications. J Comput Phys. 2015;281:787–805.
22. Huang X, Fang ZW, Sun HW, Zhang CH. A circulant preconditioner for the Riesz distributed-order space-fractional diffusion equations. Linear Multilinear Algebra. 2020;70(16):3081–96.
23. Tilli P. A note on the spectral distribution of Toeplitz matrices. Linear Multilinear Algebra. 1998;45(2-3):147–59.
24. Tyrtyshnikov EE, Zamarashkin NL. Spectra of multilevel Toeplitz matrices: advanced theory via simple matrix relationships. Linear Algebra Appl. 1998;270:15–27.
25. Barbarino G. A systematic approach to reduced GLT. BIT Numer Math. 2022;62(3):681–743.
26. Serra-Capizzano S. The GLT class as a generalized Fourier analysis and applications. Linear Algebra Appl. 2006;419(1):180–233.
27. Barbarino G, Serra-Capizzano S. Non-Hermitian perturbations of Hermitian matrix-sequences and applications to the spectral analysis of the numerical approximation of partial differential equations. Numer Linear Algebra Appl. 2020;27(3):e2286.
28. Serra-Capizzano S. More inequalities and asymptotics for matrix-valued linear positive operators: the noncommutative case. Oper Theory Adv Appl. 2002;135:293–315.
29. Serra-Capizzano S. Generalized locally Toeplitz sequences: spectral analysis and applications to discretized partial differential equations. Special issue on structured matrices: analysis, algorithms and applications. Linear Algebra Appl. 2003;366:371–402.
30. Garoni C, Manni C, Pelosi F, Speleers H. Spectral analysis of matrices resulting from isogeometric immersed methods and trimmed geometries. Comput Methods Appl Mech Eng. 2022;400:115551.
31. Bini D, Di Benedetto F. A new preconditioner for the parallel solution of positive definite Toeplitz systems. Proceedings of the 2nd Annual ACM Symposium on Parallel Algorithms and Architectures. New York: ACM; 1990. p. 220–3.
32. Van Loan C. Computational frameworks for the fast Fourier transform. Frontiers in applied mathematics. Philadelphia, PA: SIAM; 1992.
33. Axelsson O, Lindskog G. On the rate of convergence of the preconditioned conjugate gradient method. Numer Math. 1986;48(5):499–523.

How to cite this article: Mazza M, Serra-Capizzano S, Sormani RL. Algebra preconditionings for 2D Riesz distributed-order space-fractional diffusion equations on convex domains. Numer Linear Algebra Appl. 2023;e2536. https://doi.org/10.1002/nla.2536